

PAPER • OPEN ACCESS

A universal macroscopic theory of surface plasma waves and their losses

To cite this article: Hai-Yao Deng 2019 *New J. Phys.* **21** 043055

View the [article online](#) for updates and enhancements.



PAPER

A universal macroscopic theory of surface plasma waves and their losses

OPEN ACCESS

RECEIVED

21 August 2018

REVISED

11 March 2019

ACCEPTED FOR PUBLICATION

27 March 2019

PUBLISHED

30 April 2019

Hai-Yao Deng E-mail: haiyao.deng@gmail.com

School of Physics, University of Exeter, EX4 4QL Exeter, United Kingdom

National Graphene Institute, University of Manchester, Booth St E, Manchester M13 9PL, United Kingdom

Keywords: surface plasmon, charge density waves, interface and surface, electron dynamics, dynamical instability

Original content from this work may be used under the terms of the [Creative Commons Attribution 3.0 licence](https://creativecommons.org/licenses/by/4.0/).

Any further distribution of this work must maintain attribution to the author(s) and the title of the work, journal citation and DOI.



Abstract

Recently, we have revealed an intrinsic instability of metals due to surface plasma waves (SPWs) and raised the prospect of using it to create lossless SPWs. The counter-intuitive nature of this finding prompts one to ask, why had not this instability been disclosed before, given the long history of this subject? If this instability does exist, how far is it from reality? The present work is devoted to answering these questions. To this end, we derive a unified macroscopic theory of SPWs that applies to any type of electron dynamics, be they local or non-local, classical or quantum-mechanical. In light of this theory, we analyze the behaviors of SPWs according to several electron dynamics models, including the widely used local dielectric model, the hydrodynamic model and the specular reflection model, in addition to the less common semi-classical model. We find that, in order to unveil the instability, one must (i) self-consistently treat surface effects without any of the usually imposed auxiliary conditions and (ii) include translation symmetry breaking effects in electron dynamics. As far as we are concerned, none existing work had fulfilled both (i) and (ii). To assess the possibility of realizing the instability, we analyze two very important factors: the dielectric interfacing the metal and inter-band transitions, which both were ignored in our recent work. Whereas inter-band absorption—together with Landau damping—is shown adverse to the instability, a dielectric brings it closer to occurrence. One may even attain it in common plasmonic materials such as silver under not so tough conditions.

1. Introduction

Electron density ripples propagating along metal surfaces, known as surface plasma waves (SPWs), have been intensively pursued as a promising enabler of nano photonics [1–4]. A fundamental issue hampering further progress is concerned with energy losses [5]. SPWs lose energy fast due to Joule heating, Landau damping and inter-band absorption alongside others such as radiation losses [5]. It has been suggested that these losses—especially those due to Landau damping—are intrinsic and cannot be significantly reduced without the addition of external gain medium [5–9]. They would ultimately handicap the functionalities of SPWs [5, 6].

Our recent work [10–12] challenged the above view and found that, thanks to an incipient instability, the losses may well be reduced to any level without taking energy from outside. A critical point was shown to exist at $\gamma_0\tau = 1$, where τ^{-1} is the thermal electronic collision rate and γ_0 is a positive-definite quantity. At the critical point, the energy released from the Fermi sea—at rate γ_0 —just compensates for the dissipation due to electronic collisions and SPWs become lossless [12]. This instability was revealed through a semi-classical model (SCM, based on Boltzmann's transport equation) of SPWs. Given the highly counter-intuitive nature of this possibility and the long history on this subject dated back to late 1950s [13], the following questions must then be answered: *Why has the criticality not been discovered in earlier work and what is missing in those work?* While it is not widely used in the study of SPWs, the SCM had certainly been considered before [14, 15]. Yet nobody had claimed lossless SPWs.

The main purpose of the present paper is to answer the above question. Our strategy is to construct a universal theory of SPWs that is applicable to any type of electron dynamics, be they local or non-local, classical or quantum-mechanical. In light of this theory, the properties of SPWs are then analyzed with several common electron dynamics models, including the local dielectric model (DM) [13], the classical hydrodynamic model (HDM) [16–19] and the specular reflection model (SRM) [20–22] in addition to the SCM. The chief result obtained through this analysis is that, in order to unveil the instability, (i) a SPW theory must self-consistently deal with physical surfaces, and (ii) translation symmetry breaking effects must be included in the electron dynamics. Amongst these models, only the SCM is capable of (ii), but previous work based on the SCM had all failed with respect to (i). This explains why the existing work had failed to hit upon the possibility of lossless SPWs.

In existing work based on non-local models, auxiliary conditions have usually been imposed [23–26], mostly assuming no normal current on surfaces, as in the hard-wall picture adopted in computational studies [27–30]. From a conceptual point of view, however, these conditions are obviously incompatible with local models and arise only due to an incomplete description of physical surfaces [31]. We will show that the conventional treatment of SPWs via auxiliary conditions does not recover the standard textbook SPWs in the local models. We prescribe a simple yet complete macroscopic description of physical surfaces, which remedies the conceptual deficiency and allows to derive a universal SPW theory accounting for surface effects self-consistently.

As a secondary purpose, we wish to address an experimentally interesting issue, that is, *how far is the instability from reality and how can it be achieved?* In general, τ^{-1} is comparable to the characteristic plasma frequency ω_p , even in defect-free materials and at zero temperature [32]. This is because τ^{-1} is the collision rate at the SPW frequency, which is in the order of a few eVs in metals and thus effects as an effective high temperature of tens of thousands of Kelvins opening up a large phase volume for electron scattering. One then expects $\gamma_0\tau < 1$ usually. In order to devise a practically useful method of enhancing γ_0 , we employ our theory to analyze two important factors affecting γ_0 : a dielectric interfacing the metal supporting SPWs and inter-band transition effects, which were ignored in [10–12]. We find that, inter-band absorption (as well as Landau damping) strongly reduces γ_0 , whereas topping a dielectric can significantly increase γ_0 . In this way the instability may well be in reach in a single crystal of silver.

This paper is organized as follows. We develop a universal macroscopic SPW theory in the next section and apply it to the DM, the HDM and the SRM in section 4. Section 3 includes a discussion of a phenomenological approach to inter-band transition effects to make the paper self-contained. Section 5 is devoted to a thorough treatment of SPWs within the SCM. Dielectric and inter-band effects are analyzed. We assess the possibility of creating lossless SPWs by the SCM and conclude the paper in section 7. In appendices A and B, we discuss some historical misconceptions regarding the SPWs in the HDM and the SRM, respectively.

2. Universal theory of SPWs

In this section, we present a general theory of charge density waves in semi-infinite metals (SIMs). Extension to systems of other geometries is straightforward and will be considered elsewhere. The theory is formulated in terms of universal physical concepts and makes no resort to the particulars of electron dynamics. It is a macroscopic theory, thus valid as long as the thickness (d_s , typically a few lattice constants) of the microscopic surface layer, which forms between the vacuum and the bulk metal, is much smaller than the SPW wavelength Λ . In this paper, by ‘macroscopic’ we always mean $d_s/\Lambda \ll 1$, with no regard to electron dynamics.

Retardation effects are neglected throughout this paper, which is reasonable provided the SPW phase velocity is much less than the speed of light in vacuum.

2.1. Macroscopic description of surfaces

The SIM under consideration is assumed to occupy the region $z \geq 0$ and bounded by a flat interface/surface macroscopically located at $z = 0$. The other half space is either the vacuum or a dielectric with dielectric constant ϵ_d , see figure 1. The surface is assumed flat on the macroscopic scale so that translation symmetry is preserved along the surface, but it may be ragged on the scale of Fermi wavelength and therefore can diffusively scatter electron waves. We shall use the vector $\mathbf{x} = (\mathbf{r}, z)$ to denote a point in space, where $\mathbf{r} = (x, y)$ is the planar projection of \mathbf{x} . Further, $\mathbf{x}_0 = (\mathbf{r}, 0)$ denotes a point on the surface and t denotes time.

In a macroscopic description of SPWs, one usually considers the metal as a medium for an electromagnetic field and seeks surface localized (polariton) solutions of the governing Maxwell’s equations [33]. The procedure is to write down the waves for (an infinite metal) on the metal side and those (for an infinite dielectric) on the dielectric side, and then invoke conditions to match those waves at the surface. With local dynamics, the usual Maxwell’s boundary conditions would do the job. With non-local dynamics, however, they are insufficient. Historically, auxiliary conditions—mostly assuming zero normal current at the surface [14, 15, 17, 25]—have been invented as a remedy since 1950s [23], which however treat the symptoms not the cause. The cause is a conceptual deficiency in the knowledge of surfaces [31]. Considering that a real microscopic surface can hardly

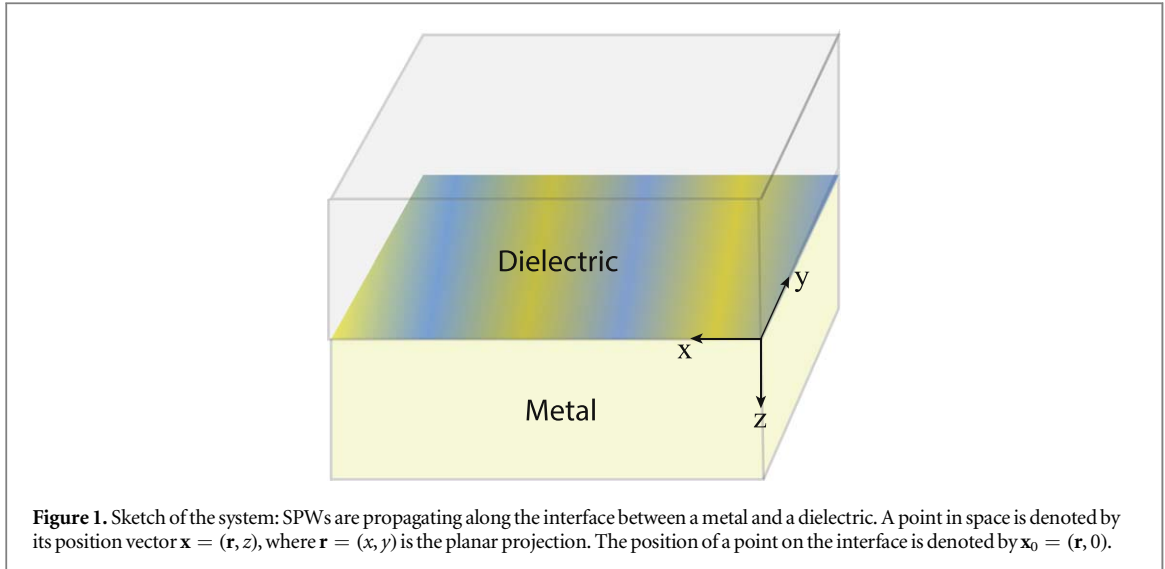


Figure 1. Sketch of the system: SPWs are propagating along the interface between a metal and a dielectric. A point in space is denoted by its position vector $\mathbf{x} = (\mathbf{r}, z)$, where $\mathbf{r} = (x, y)$ is the planar projection. The position of a point on the interface is denoted by $\mathbf{x}_0 = (\mathbf{r}, 0)$.

be specified even for the simplest material due to preparation procedures, one might deem it hopeless to have a complete description. The following elementary analysis suggests otherwise.

Let us imagine bringing two materials (A and B) in contact, and an interfacial layer of thickness d_s —in the order of a few lattice constants—shall form in between. We may characterize this layer by a surface potential ϕ_s , which should quickly decay to zero in the bulk regions outside the interfacial layer. The exact microscopic profile of the layer varies from one case to another and can hardly be known *a priori*. Despite this, we may still write down a generic form for the electric current density $\mathbf{j}(\mathbf{x}, t)$ in the whole system including the interfacial layer. To this end, we observe that in the bulk regions where ϕ_s vanishes, the form of $\mathbf{j}(\mathbf{x}, t)$ can be completely specified with the respective dynamic equations for the infinite materials, apart from some parameters (such as the *Fuchs* parameter, see section 5) that encode the effects of surface scattering on the electron waves. Let us denote by $\mathbf{J}_{A/B}(\mathbf{x}, t)$ the forms of $\mathbf{j}(\mathbf{x}, t)$ in the bulk region of A/B . Microscopically, \mathbf{j} evolves from \mathbf{J}_A in the bulk region of A , through a rapid variation in the interfacial layer, to \mathbf{J}_B in the bulk region of B . Formally, we can write for the μ th component of the current density that $j_{\mu}(\mathbf{x}, t) = J_{A,\mu}(\mathbf{x}, t)w_{\mu}(z) + J_{B,\mu}(\mathbf{x}, t)(1 - w_{\mu}(z))$, where the profile functions $w_{\alpha}(z)$ approach unity in the bulk region of A and zero in that of B . The exact profile of $w_{\mu}(z)$ depends on the microscopic details of the interfacial layer. On the scale of λ , however, the interfacial layer appears infinitely thin and $w_{\alpha}(z)$ reduce to the Heaviside step function $\Theta(z)$, where $\Theta(z \geq 0) = 1$ and $\Theta(z < 0) = 0$, in a macroscopic theory. One thus ends up with

$$\mathbf{j}(\mathbf{x}, t) = \mathbf{J}_A(\mathbf{x}, t)\Theta(z) + \mathbf{J}_B(\mathbf{x}, t)(1 - \Theta(z)). \quad (1)$$

This holds valid for any $w_{\mu}(z)$ and is thus a general and complete macroscopic description of a physical interface, as long as a perturbation on one side does not cause significant responses on the other.

To recapitulate, equation (1) elegantly captures two importance physical consequences of an interface: the rapid variation of the current density through the step function $\Theta(z)$ and the surface scattering effects on electron dynamics through the parameters contained in the bulk forms. These scattering effects—including the symmetry breaking effects—have been ignored in most models except for the SCM. In general \mathbf{J}_A and \mathbf{J}_B are not equal on the interface, as is certainly the case for local dynamics models, and charges accumulate in the interfacial layer. Such capacitive effects would be mistakenly erased under auxiliary conditions, which often dictate continuity of current across the interface, e.g. the vanishing of normal current at the metal–vacuum interface.

2.2. Charge density waves

Now we derive the equations of motion for the charge density $\rho(\mathbf{x}, t) = en(\mathbf{x}, t)$, where e denotes the charge of an electron and $n(\mathbf{x}, t)$ is the deviation from the mean electron density n_0 , in the SIM. Our starting point is the equation of continuity. Specifying equation (1) to the SIM, we have $\mathbf{j}(\mathbf{x}, t) = \Theta(z)\mathbf{J}(\mathbf{x}, t)$, where $\mathbf{J}(\mathbf{x}, t)$ is the current density in the metal. The equation of continuity then reads

$$\mathcal{D}_t \rho(\mathbf{x}, t) + \partial_x \cdot \mathbf{j}(\mathbf{x}, t) = 0, \quad \mathcal{D}_t = \tau^{-1} + \partial_t.$$

Here we have included a global relaxation term $-\rho(\mathbf{x}, t)/\tau$ to account for the thermal relaxation of non-equilibrium charges due to microscopic electronic collisions driving the system toward thermodynamic equilibrium. In terms of $\mathbf{J}(\mathbf{x}, t)$, this equation becomes

$$\mathcal{D}_t \rho(\mathbf{x}, t) + \partial_{\mathbf{x}} \cdot \mathbf{J}(\mathbf{x}, t) = -\Theta'(z) J_z(\mathbf{x}_0, t), \quad (2)$$

where $\Theta'(z) = \partial_z \Theta(z)$. The right-hand term of this equation signifies the capacitive effects, which is critical in the energy conversion process but had been overlooked until our recent work [12]. This term was also noticed by Fetter in studying the edge plasmon in two-dimension systems [19].

Without loss of generality, we may assume a quasi-plane wave for the fields and write $\rho(\mathbf{x}, t) = \rho(z) e^{i(\mathbf{k} \cdot \mathbf{r} - \omega t)}$ and similarly for $\mathbf{J}(\mathbf{x}, t)$ and the electric field $\mathbf{E}(\mathbf{x}, t)$, where the wave vector $\mathbf{k} = (k \geq 0, 0)$ is directed along the positive x -axis for the sake of definiteness. In general the frequency $\omega = \omega_s - i\gamma$ is complex. The relation between ω and k is determined by the wave equations to be established in what follows. Equation (2) thus becomes

$$-i\bar{\omega} \rho(z) + \nabla \cdot \mathbf{J}(z) = -J_z(0) \Theta'(z), \quad \nabla = (i\mathbf{k}, \partial_z), \quad (3)$$

where $\bar{\omega} = \omega + i/\tau$ and $J_z(\mathbf{x}_0, t) = J_z(0) e^{i(\mathbf{k} \cdot \mathbf{r} - \omega t)}$. We shall write $\bar{\omega} = \omega_s + i\gamma_0$, so that

$$\gamma = 1/\tau - \gamma_0 \quad (4)$$

by definition. We shall see that γ_0 is negative in all models except for the SCM, in which it is positive-definite thanks to a fundamental physical reason.

For linear responses, $\mathbf{J}(z)$ can be related to $\mathbf{E}(z)$ as follows

$$J_\mu(z) = \sum_{\nu=x,y,z} \int dz' \sigma_{\mu\nu}(z, z', \omega) E_\nu(z'), \quad (5)$$

where $\sigma_{\mu\nu}(z, z', \omega)$ is the conductivity tensor. Considering that $\mathbf{E}(z)$ linearly depends on $\rho(z)$, we can define a linear operator $\hat{\mathcal{H}}$ with kernel $\mathcal{H}(z, z')$ so that

$$\hat{\mathcal{H}}\rho(z) = \int dz' \mathcal{H}(z, z') \rho(z') = -i\bar{\omega} \nabla \cdot \mathbf{J}(z). \quad (6)$$

It is easy to show that

$$\mathcal{H}(z, z') = i\bar{\omega} \sum_{\mu\nu} \int_0^\infty dz'' \nabla_\mu \sigma_{\mu\nu}(z, z'', \omega) \nabla''_\nu V_{\mathbf{k}}(z'' - z'),$$

where $\nabla'' = (i\mathbf{k}, \partial_{z''})$ and $V_{\mathbf{k}}(z)$ is the \mathbf{k} th Fourier component of the Coulomb interaction $V(\mathbf{x}) = 1/|\mathbf{x}|$. Now equation (3) can be transformed into

$$(\hat{\mathcal{H}} - \bar{\omega}^2) \rho(z) = S \Theta'(z), \quad S = i\bar{\omega} J_z(0). \quad (7)$$

Note that S does not depend on z . Since $\rho(z)$ is defined only for $z \geq 0$, we can introduce a cosine Fourier transform

$$\rho(z) = \frac{2}{\pi} \int_0^\infty dq \rho_q \cos(qz).$$

In terms of ρ_q , equation (7) can be rewritten as

$$\int_0^\infty dq' (\mathcal{H}(q, q') - \bar{\omega}^2 \delta(q - q')) \rho_{q'} = S. \quad (8)$$

Here

$$\mathcal{H}(q, q') = \frac{2}{\pi} \int_0^\infty dz \int_0^\infty dz' \cos(qz) \mathcal{H}(z, z') \cos(q'z')$$

is the matrix element between the cosine waves. Finally, we close equation (8) by the fact that $J_z(0)$ and hence S are also linear functionals of ρ_q . We can thus write

$$S = \int_0^\infty dq \frac{G(\mathbf{K}, \omega)}{K^2} \rho_q, \quad (9)$$

where $\mathbf{K} = (k, 0, q)$, $K^2 = k^2 + q^2$ and G is a kernel given by

$$G(\mathbf{K}, \omega) = \frac{2\bar{\omega}}{i\pi} \int_0^\infty dz \int_0^\infty dz' \cos(qz) \sigma_{\mu\nu}(0, z', \omega) \nabla'_\nu V_{\mathbf{k}}(z' - z).$$

As a key result of this paper, equations (8) and (9) constitute a complete description of self-sustained charge density waves in SIMs. Their basic structures are valid regardless of the underlying electron dynamics encoded in \mathcal{H} and G .

2.3. Universal secular equation for SPWs

Equation (8) is an inhomogeneous linear equation with a source term. Equations of this type generally admit of two classes of solutions, depending on whether S vanishes or not. Solutions with $S = 0$ represent nothing but the bulk plasma waves, while those with $S \neq 0$ represent localized waves, i.e. SPWs in our system. The spectra of

these two classes generally do not overlap. Had we imposed auxiliary boundary conditions as is usually done in the literature, SPWs would not exist at all.

To find the ‘secular’ equation for SPWs, we wish to make a simplification, which is not necessary but will make the resulting expressions more transparent. To this end, let us look at some general properties of $\sigma_{\mu\nu}(z, z', \omega)$. For an infinite system without boundaries, the translational symmetry is preserved along z -axis as well as along the surface plane, in which case $\sigma_{\mu\nu}$ only depends on $z - z'$. For SIMs, however, that symmetry is broken and $\sigma_{\mu\nu}$ must in general depend on z and z' separately. It shall prove useful to decompose $\sigma_{\mu\nu}$ into two parts, $\sigma_{b,\mu\nu}$ and $\sigma_{s,\mu\nu}$, where $\sigma_{b,\mu\nu}$ is defined to be that of the infinite system and depends only on $z - z'$ while $\sigma_{s,\mu\nu}$ signifies pure surface effects. Namely,

$$\sigma_{\mu\nu}(z, z', \omega) = \sigma_{b,\mu\nu}(z - z', \omega) + \sigma_{s,\mu\nu}(z, z', \omega).$$

Accordingly, \mathcal{H} and G also each contain two parts arising from $\sigma_{b,\mu\nu}$ and $\sigma_{s,\mu\nu}$, respectively. Let us then write $\mathcal{H} = \mathcal{H}_b + \mathcal{H}_s$. Now that it reflects on the properties of plasma waves of an infinite system, \mathcal{H}_b must be diagonal in the q -space, i.e. $\mathcal{H}_b(q, q') = \Omega^2(K, \omega)\delta(q - q')$, where $\Omega(K, \omega)$ is a frequency that only depends on K . By definition, one can easily show that the dielectric function of an infinite system is given by

$$\epsilon(K, \omega) = 1 - \frac{\Omega^2(K, \omega)}{\bar{\omega}^2}. \quad (10)$$

As for \mathcal{H}_s , it gives rise to scattering of plasma waves. Nevertheless, for bulk waves the scattering due to a surface should be insignificant and may be treated perturbatively, as we did in [10, 11]. To the lowest order in this perturbation, we may simply put

$$\mathcal{H}(q, q') = \Omega^2(K, \omega)\delta(q - q'). \quad (11)$$

This expression contains complete information of bulk plasma waves. As expected, the zeros of $\epsilon(K, \omega)$ give the dispersion $\epsilon_b(K)$ of these waves.

We analogously write $G = G_b + G_s$. Note that via equation (9) G_b determines J_z at the point $z = 0$ in a infinite system, for which, however this point is none more special than any other points. Thus, G_b can only be a constant that does not depend on q and it is therefore purely due to the local part of $\sigma_{b,\mu\nu}(z - z')$. This part must be isotropic for the jellium model and it can be written as $\delta_{\mu\nu}\delta(z - z')\sigma(\omega)$, where $\delta_{\mu\nu}$ is the Kronecker symbol and $\sigma(\omega)$ is to be discussed further. It follows that $G_b = -4i\bar{\omega}\sigma(\omega)k\beta$, where we have taken into account the effect of the dielectric via the factor $\beta = 2\epsilon_d/(1 + \epsilon_d)$; see details below. We now obtain

$$G(\mathbf{K}, \omega) = -4i\bar{\omega}\sigma(\omega)k\beta + G_s(\mathbf{K}, \omega). \quad (12)$$

We see that G_s describes translation symmetry breaking effects. As to be seen later, it is missing from the DM, the HDM and the SRM. The positive-definiteness of γ_0 arises solely through this term and therefore cannot be captured in these models.

For SPWs, $S \neq 0$. Inserting equation (11) in (8) and using (9), we find

$$\epsilon_s(k, \omega) = 1 - \int_0^\infty \frac{dq}{K^2} \frac{G(\mathbf{K}, \omega)}{\Omega^2(K, \omega) - \bar{\omega}^2} = 0, \quad (13)$$

which determines the SPW frequency ω_s and damping rate γ as a function of k . This is another key result of this paper. The SPW charge density is obtained as

$$\rho_q = \frac{S}{\Omega^2(K, \omega) - \bar{\omega}^2} = \frac{S}{\bar{\omega}^2} \left(-\frac{1}{\epsilon(K, \omega)} \right). \quad (14)$$

The resulting $\rho(z)$ is peaked about the surface.

Equations (13) and (14) constitute a universal description of SPWs. They are valid irrespective of the underlying electron dynamics, which enter only through $\epsilon(K, \omega)$ and $G(\mathbf{K}, \omega)$.

2.4. Dielectric effects

Let us place a dielectric with dielectric constant ϵ_d —which can be complex—on the side $z < 0$. The electrostatic fields are affected by this dielectric, which can be calculated with the method of mirror charges. Let the mirror charge density in the dielectric be $\rho_d(\mathbf{x}, t) = \rho_d(z)e^{i(\mathbf{k}\cdot\mathbf{r} - \omega t)}$. It is easy to show that [34]

$$\rho_d(z < 0) = -\frac{\epsilon_d - 1}{\epsilon_d + 1}\rho(-z). \quad (15)$$

The electrostatic potential $\phi(\mathbf{x}, t) = \phi(z)e^{i(\mathbf{k}\cdot\mathbf{r} - \omega t)}$, obeying Poisson’s equation $\partial_x^2\phi(\mathbf{x}, t) + 4\pi(\rho(\mathbf{x}, t) + \rho_d(\mathbf{x}, t)) = 0$, is then obtained as

Table 1. A comparison of various models in light of the present universal theory of SPWs. DM: classical dielectric model. HDM: hydrodynamic model. SRM: specular reflection model. SCM: semi-classical model. For the sake of simplicity, $\epsilon_p = 0$ and $\epsilon_d = 1$ have been used in the expressions given in this table. $\mathbf{K} = (k, 0, q)$. $G_0 = (k/\pi)\omega_p^2$, where ω_p denotes the characteristic plasma frequency of the metal. $\mathbf{F} = (m/2\pi\hbar)^3 \int d^3\mathbf{v}(-e^2 f'_0) \mathbf{v}(\mathbf{K} \cdot \mathbf{v}/\bar{\omega})^2 (1 - \mathbf{K} \cdot \mathbf{v}/\bar{\omega})^{-1}$, where \mathbf{v} is the velocity of electrons of mass m . $\epsilon(\mathbf{K}, \omega)$ is the dielectric function of the infinite system, whose zeros give the dispersion of bulk plasma waves. SPWs are determined by this secular equation: $\epsilon_s = 1 + \int_0^\infty \frac{dq}{k^2} \frac{G(\mathbf{K}, \omega)}{\bar{\omega}^2} \frac{1}{\epsilon(\mathbf{K}, \omega)} = 0$. The solution to this equation is written as $\omega = \omega_s - i\gamma$. In the SCM, an extra contribution γ_s arises due to symmetry breaking effects contained in G_s . Very interestingly, $\gamma_0 = \gamma_s - \gamma_{\text{Landau}} - \gamma_{\text{interband}}$ cannot be negative.

Quantity	DM	HDM	SRM	SCM
Symmetry breaking effects	No	No	No	Yes
$\Omega^2(K, \omega)$	ω_p^2	$\Omega_{\text{HDM}}^2 = \omega_p^2 + Bv_F^2 K^2$	$\omega_p^2 + \frac{4\pi\bar{\omega}\mathbf{K}\cdot\mathbf{F}}{K^2}$	$\omega_p^2 + \frac{4\pi\bar{\omega}\mathbf{K}\cdot\mathbf{F}}{K^2}$
$G(\mathbf{K}, \omega)$	G_0	G_0	G_0	$G_0 + G_s$
$\epsilon(\mathbf{K}, \omega)$	$1 - \frac{\omega_p^2}{\bar{\omega}^2}$	$1 - \frac{\Omega_{\text{HDM}}^2}{\bar{\omega}^2}$	$1 - \frac{\Omega^2}{\bar{\omega}^2}$	$1 - \frac{\Omega^2}{\bar{\omega}^2}$
Damping rate γ	$\tau^{-1} + \gamma_{\text{interband}}$	$\tau^{-1} + \gamma_{\text{interband}}$	$\tau^{-1} + \gamma_{\text{interband}} + \gamma_{\text{Landau}}$	$\tau^{-1} + \gamma_{\text{interband}} + \gamma_{\text{Landau}} - \gamma_s$

$$\phi(z) = \frac{2\pi}{k} \int_{-\infty}^{\infty} dz' e^{-k||z-z'||} (\rho(z') + \rho_d(z')). \quad (16)$$

In the metal, where $z \geq 0$, the electric field $\mathbf{E}(z) = -\nabla\phi(z) = (E_x(z), 0, E_z(z))$ then follows as

$$E_x(z) = -i \int_0^\infty dq \frac{4k\rho_q}{K^2} (2 \cos(qz) - \beta e^{-kz}) \quad (17)$$

and

$$E_z(z) = \int_0^\infty dq \frac{4k\rho_q}{K^2} \left(2 \frac{q}{k} \sin(qz) - \beta e^{-kz} \right), \quad (18)$$

where β has been given in the above. See that $E_z(0)$ and hence G_b are enhanced by the factor β , which is why this factor appears in equation (12). Physically this is because the surface sits between the charges in the metal and those in the dielectric and spatially separates them.

3. Inter-band transition effects

The dynamics models to be considered in the next two sections only describe the currents from electrons in the conduction band. Realistically, valence electrons can also contribute by virtual inter-band transitions. In this paper, for the sake of simplicity, we account for these inter-band transition effects by a phenomenological approach [35–37]. The observation is that, valence electrons are usually tightly held to their host atoms and the energy bands are largely non-dispersion, and thus their electrical responses are mostly local and not susceptible to the presence of boundaries. We may then describe this response by a local conductivity function $\sigma_p(\omega)$, so that the electrical current density due to the valence electrons is given by

$$\mathbf{J}_p(z) = \sigma_p(\omega)\mathbf{E}(z). \quad (19)$$

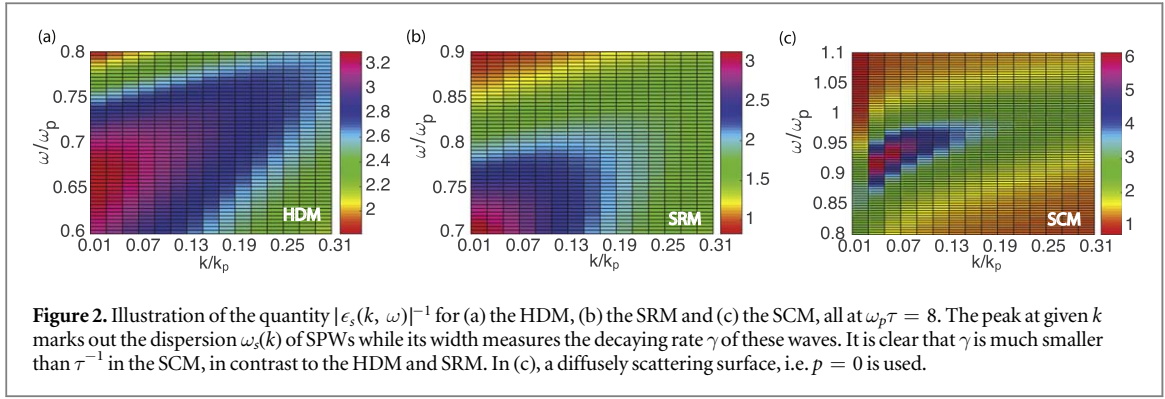
Usually $\sigma_p(\omega)$ may be modeled in the Lorentz form. It is related to the inter-band dielectric function by $\epsilon_p(\omega) = 4\pi i\sigma_p(\omega)/\bar{\omega}$, which can be measured for example by means of ellipsometry or computed by density functional theory. $\epsilon_p(\omega)$ contains a real part $\epsilon_{pr}(\omega)$ and an imaginary part $\epsilon_{pi}(\omega)$. While $\epsilon_{pr}(\omega)$ acts to shield the conduction electrons, $\epsilon_{pi}(\omega)$ —which is always positive—leads to inter-band absorption. Being basically an atomic property, ϵ_p is not sensitive to temperature.

4. SPWs in DM, HDM and SRM

While the theory established in section 2 is universal, the behaviors of SPWs do depend on electron dynamics through $\epsilon(K, \omega)$ and $G(\mathbf{K}, \omega)$. In this section, we apply the theory to examine SPWs within several common electron dynamics models: the DM, the HDM and the SRM. SPWs in the SCM will be thoroughly treated in the next section. We show that the usually quoted SPW solution in the HDM is false and clarify the origin of SPWs in the SRM. A summary of this analysis is tabulated in table 1, and a comparison between the properties of the SPWs according to these models is illustrated in figure 2, where the quantity $1/|\epsilon(k, \omega)|$ is mapped out.

4.1. Local DM

This is the standard model for SPWs. Unlike other models, it does not require and is incompatible with any auxiliary conditions. Here we reproduce by our theory the well-known properties of SPWs in this model.



According to the DM, the current density due to conduction electrons is given by

$$\mathbf{J}_{\text{DM}}(z) = \sigma_{\text{DM}}(\omega)\mathbf{E}(z), \quad \sigma_{\text{DM}}(\omega) = \frac{i}{\bar{\omega}} \frac{\omega_p^2}{4\pi}, \quad (20)$$

where $\omega_p = \sqrt{4\pi n_0 e^2/m}$ is the characteristic plasma frequency of the metal with m and e being the effective mass and charge of an electron, respectively. The total current density $\mathbf{J}(z)$ then is

$$\mathbf{J}(z) + \mathbf{J}_{\text{DM}}(z) = (\sigma_{\text{DM}}(\omega) + \sigma_p(\omega))\mathbf{E}(z),$$

yielding $\sigma(\omega) = \sigma_{\text{DM}}(\omega) + \sigma_p(\omega)$. From equation (6) one finds Ω^2 dispersionless, given as

$$\Omega_0^2(\omega) = \omega^2 - \bar{\omega}^2 \epsilon_p(\omega).$$

Bulk plasma waves. Equating Ω_0^2 with $\bar{\omega}^2$ yields the frequency $\omega_{b,\text{DM}}$ and damping rate $\gamma_{b,\text{DM}}$ for bulk plasma waves. For $\omega_p\tau \rightarrow \infty$ and assuming $\epsilon_p(\omega)$ independent of ω , they are given by

$$\omega_{b,\text{DM}} = \frac{\omega_p}{\sqrt{1 + \epsilon_{pr}}}, \quad \gamma_{b,\text{DM}}/\omega_{b,\text{DM}} = \frac{1}{\omega_{b,\text{DM}}\tau} + \frac{1}{2} \frac{\epsilon_{pi}}{1 + \epsilon_{pr}}.$$

Note that bulk waves bear no dielectric effects, i.e. no dependence on ϵ_d . The damping rate $\gamma_{b,\text{DM}}$ arises due to thermal collisions and inter-band absorption.

SPWs. The electrical conductivity is purely local and thus $G_s = 0$. As such, $G(\mathbf{K}, \omega)$ becomes

$$G_0 = (k\beta/\pi)\Omega_0^2(\omega).$$

Substituting this into equation (13), we immediately arrive at the often quoted frequency $\omega_{s,\text{DM}}$ and damping rate $\gamma_{s,\text{DM}}$ for SPWs. Neglecting absorption in the dielectric, i.e. assuming real ϵ_d , we find

$$\omega_{s,\text{DM}} = \frac{\omega_p}{\sqrt{1 + \epsilon_d + \epsilon_{pr}}}, \quad \frac{\gamma_{s,\text{DM}}}{\omega_{s,\text{DM}}} = \frac{1}{\omega_{s,\text{DM}}\tau} + \frac{1}{2} \frac{\epsilon_{pi}}{1 + \epsilon_d + \epsilon_{pr}}.$$

In this model, the SPW charge density is completely localized on the surface, $\rho(z) = \rho_s \Theta'(z)$, where $\rho_s = S/(\Omega_0^2 - \bar{\omega}^2)$ gives the areal charge density. See that the dielectric tends to reduce the SPW damping rate.

Traditionally [38], the above results have been obtained by treating the metal as a simple dielectric with dielectric constant $\epsilon(\omega) = 1 - \Omega_0^2/\bar{\omega}^2$. Then exponentially decaying electromagnetic (EM) waves (or electrostatic potentials in the quasi-static limit) are written down on the metal and the dielectric sides, and Maxwell's boundary conditions are used to match the waves to obtain the above frequency and damping rate of SPWs. Our theory works directly with charge density rather than EM waves. The two approaches are equivalent.

4.2. Hydrodynamic model (HDM)

The DM assumes a purely local relation between the current density and the electric field. The HDM extends the DM by inclusion of leading-order non-local corrections. Recently, this model has attracted lots of attention in plasmonics and quantum forces [39–41]. It has also been synergized with density functional theory in the quantum HDM [42–45] to study local plasmon resonances on metal particles.

In the HDM, Ω^2 includes leading-order dependence on K and is given by

$$\Omega_{\text{HDM}}^2 = \Omega_0^2 + K^2 v_0^2,$$

where v_0 is a parameter. The dielectric function¹ then reads $\epsilon_{\text{HDM}} = 1 - \Omega_{\text{HDM}}^2/\bar{\omega}^2$. The bulk waves are similar to those in the DM except for some dispersion with K .

As in the DM, no symmetry breaking effects are included in the HDM. $G(\mathbf{K}, \omega)$ is then the same as that for the DM. Now equation (13) transforms into the following

$$1 + \frac{k\beta}{\pi} \frac{\Omega_0^2}{\bar{\omega}^2} \int_0^\infty \frac{dq}{K^2} \frac{1}{\epsilon_{\text{HDM}}} = 0, \quad (21)$$

which determines the SPWs in the HDM by our theory. Note that the integrand contains no poles or resonances near the solutions, as the SPW spectra are always gapped from the bulk wave spectra gratifying $\epsilon_{\text{HDM}} = 0$. For $v_0 = 0$, the HDM reduces to the DM and so do the SPWs, as expected. With $\epsilon_d = 0$ and $\epsilon_p = 0$, the equation simplifies to

$$1 + \frac{k}{\pi} \int_{-\infty}^\infty \frac{dq}{K^2} \frac{1}{\epsilon_{\text{HDM}}} = 0, \quad (22)$$

where we have used the fact that ϵ_{HDM} is even in q and that $\omega_p^2/\bar{\omega}^2 \approx 2$ for the solutions to this equation. As shown in appendix A, it leads to a linear dispersion of ω_s versus k . As in the DM, the SPW damps due to thermal collisions and inter-band absorption, at rate $\gamma_{s,\text{HDM}} \approx \gamma_{s,\text{DM}}$ apart from some dispersion effects.

In the literature, the condition that $J_z(0) = 0$ is usually imposed in the HDM [15, 17]. This would mean $S = 0$ and therefore would exclude any SPWs according to our theory. Nevertheless, SPWs have been claimed to exist under this condition. In what follows we briefly show that this claim is false, more details to be found in appendix A.

For illustration, we take $\epsilon_p = 0$ and $\epsilon_d = 0$. Impose $S = 0$ and the wave equation becomes $(\Omega_{\text{HDM}}^2 - \bar{\omega}^2)\rho_q = 0$, or equivalently in the real space

$$(\bar{\omega}^2 - (\omega_p^2 + v_0^2 k^2) + v_0^2 \partial_z^2)\rho(z) = 0. \quad (23)$$

The claimed SPW solution is then sought of the form $\rho(z) = \rho_0 e^{-\kappa z}$. Substituting this in the equation leads to $\bar{\omega}^2 = \omega_p^2 + v_0^2(k^2 - \kappa^2)$. Imposing $J_z(0) = 0$ gives another relation, $\omega_0^2 = v_0^2 \kappa(k + \kappa)$, which expresses the balance between the electronic pressure and the electric force at the surface. Here $\omega_0 = \omega_p/\sqrt{2}$. Those two relations specify the solution. Combined, they lead to $\bar{\omega}^2 \approx \omega_0^2 + \omega_0 \beta k$. Nevertheless, this solution does not reduce in the limit $v_0 = 0$ to the SPWs found by Ritchie with the DM. Actually, κ diverges in this limit, yielding $\int \rho(z) dz \sim \kappa^{-1} = 0$, i.e. the solution is empty of charges. This false solution is also what was observed in [14, 15, 47]. It is plausible that existing *ab initio* calculations have only observed this false solution as well [28]. A comprehensive account may merit a future study.

Although the false solution and the correct solution are conceptually disparate, their dispersion relations are quite similar, as shown in appendix A.

4.3. Specular reflection model (SRM)

A natural step to go beyond the HDM is to use the full form of Ω rather than the approximation Ω_{HDM} . Equation (22) then becomes

$$1 + \frac{k}{\pi} \int_{-\infty}^\infty \frac{dq}{K^2} \frac{1}{\epsilon(\mathbf{K}, \omega)} = 0. \quad (24)$$

This is exactly the equation established by Marusak and Ritchie in 1966 for the SRM [20]. Our derivation makes it clear that the SRM is just an extension of the HDM. From this point of view, one may also conclude that the usually claimed SPWs in the HDM are false, because they are not solutions of equation (24) in the HDM limit.

In contrast with the DM and the HDM, SPWs in the SRM can also decay via Landau damping, because of an imaginary part in Ω associated with electron-hole excitations. Thus, the SPW damping rate is $\gamma_{s,\text{SRM}} \approx \gamma_{s,\text{DM}} + \gamma_{\text{Landau}}$, see the next section for further discussion on this.

We wish to point out a logical inconsistency in the original contrivance of the SRM. There are two elements in this contrivance: (i) as nominally expected, electron waves impinging on the surface are assumed to be specularly reflected back, and (ii) a sheet of ‘fictitious’ charges exactly localized on the surface. Element (i) would mean $J_z(0) = 0$ and hence, by our theory, no SPWs would materialize. Then how do those waves come about?

¹ Note that ϵ_{HDM} differs from the bulk dielectric function that is usually quoted in the literature, which reads $1 - \omega_p^2/(\bar{\omega}^2 - K^2 v_0^2)$. This function can be easily obtained from equations (A2) and (A5) by adding an external term \mathbf{E}_{ext} to \mathbf{E} and taking $\partial_x \cdot \mathbf{E}_{\text{ext}} = 4\pi\rho_{\text{ext}}$. The dielectric function then by definition is given by $\rho_{\text{ext}}/(\rho_{\text{ext}} + \rho)$. The difference arises from two non-equivalent approaches to the HDM, see [46] for more discussions.

The answer rests with element (ii). In appendix B, we show that the fictitious charge sheet reinstates the capacitive effects lost under element (i). Actually, SPWs appear as a pole of this fictitious charge density.

As with the HDM and the DM, the SRM contains no symmetry breaking effects, i.e. G_s is absent from these models. To account for these effects, further improvement is required, leading to the SCM.

5. SPWs in the SCM

In the SCM one calculates the electric currents in terms of a distribution function $f(\mathbf{x}, \mathbf{v}, t)$ defined in the single-particle phase space. As usual, we write it as a sum of the equilibrium part $f_0(\varepsilon(\mathbf{v}))$ and the non-equilibrium part $g(\mathbf{x}, \mathbf{v}, t)$. $f_0(\varepsilon)$ is taken to be the Fermi–Dirac function at zero temperature. $\varepsilon(\mathbf{v}) = m\mathbf{v}^2/2$ is the dispersion of the conduction band. Within the relaxation time approximation and the regime of linear responses, $g(\mathbf{x}, \mathbf{v}, t) = g(\mathbf{v}, z)e^{i(\mathbf{k}\cdot\mathbf{r} - \omega t)}$ satisfies the following Boltzmann's equation

$$(\lambda^{-1} + \partial_z)g(\mathbf{v}, z) + ef'_0(\varepsilon)\mathbf{v} \cdot \mathbf{E}(z)/v_z = 0. \quad (25)$$

Here $\lambda = iv_z/\tilde{\omega}$ with $\tilde{\omega} = \tilde{\omega} - kv_x$ and $f'_0 = \partial_\varepsilon f_0(\varepsilon) = (2/m)\delta(v^2 - v_F^2)$, where m is the electron effective mass and v_F the Fermi velocity.

Physical causality [10] requires that $\gamma_0 = \text{Im}(\tilde{\omega}) \geq 0$; otherwise, reflected electron waves would come before incident waves. Together with equation (4), we may conclude that the SPW damping rate is always in short of τ^{-1} , i.e. $\gamma\tau < 1$, in non-reconcilable contrast with other models.

With $\gamma_0 \geq 0$, the general solution to equation (25) can be written as

$$g(\mathbf{v}, z) = e^{-\frac{z}{\lambda}} \left(C(\mathbf{v}) - \frac{ef'_0\mathbf{v}}{v_z} \cdot \int_0^z dz' e^{\frac{z'}{\lambda}} \mathbf{E}(z') \right), \quad (26)$$

where $C(\mathbf{v}) = g(\mathbf{v}, 0)$ is the non-equilibrium deviation on the surface to be determined by boundary conditions. We require $g(\mathbf{v}, z) = 0$ distant from the surface, i.e. $z \rightarrow \infty$. For electrons moving away from the surface, $v_z > 0$, this condition is automatically fulfilled. For electrons moving toward the surface, $v_z < 0$, it leads to

$$C(\mathbf{v}) = \frac{ef'_0\mathbf{v}}{v_z} \cdot \int_0^\infty dz' e^{z'/\lambda} \mathbf{E}(z'), \quad v_z < 0. \quad (27)$$

It follows that

$$g(\mathbf{v}, z) = \frac{ef'_0\mathbf{v}}{v_z} \cdot \int_z^\infty dz' e^{\frac{z'-z}{\lambda}} \mathbf{E}(z'), \quad v_z < 0. \quad (28)$$

To determine $C(\mathbf{v})$ for $v_z > 0$, the boundary condition at $z = 0$ has to be used, which, however, depends on surface properties. We adopt a simple picture first conceived by Fuchs [48] and then widely used in the study of for instance anomalous skin effect [49–52]. According to this picture a fraction p i.e. the *Fuchs* parameter varying between zero and unity, of the electrons impinging on the surface are specularly reflected back, i.e.

$$g(\mathbf{v}, z = 0) = p g(\mathbf{v}_-, z = 0), \quad \mathbf{v}_- = (v_x, v_y, -v_z), \quad v_z \geq 0. \quad (29)$$

This condition is identical with the condition used in [12] but differs from that in [10, 11] except for $p = 0$. It follows that

$$C(\mathbf{v}) = -p \frac{ef'_0\mathbf{v}_-}{v_z} \cdot \int_0^\infty dz' e^{-\frac{z'}{\lambda}} \mathbf{E}(z'), \quad v_z \geq 0. \quad (30)$$

Equations (26)–(30) fully specify the distribution function for the electrons.

The electrical current density due to the conduction electrons is then calculated as

$$\mathbf{J}_c(z) = (m/2\pi\hbar)^3 \int d^3\mathbf{v} e\mathbf{v}g(\mathbf{v}, z). \quad (31)$$

Note that the charge density is not given by

$$\tilde{\rho}(\mathbf{x}, t) = (m/2\pi\hbar)^3 e^{i(\mathbf{k}\cdot\mathbf{x} - \omega t)} \int d^3\mathbf{v} eg(\mathbf{v}, z).$$

The reason is simple: the as-obtained $g(\mathbf{v}, z)$ is for the bulk region and not valid on the surface, because equation (3.1) involves no surface potentials, see section 2.1. Actually, $\mathbf{J}_c(\mathbf{x}, t)$ and $\tilde{\rho}(\mathbf{x}, t)$ obey the equation

$$(\partial_t + 1/\tau)\tilde{\rho}(\mathbf{x}, t) + \partial_x \cdot \mathbf{J}_c(\mathbf{x}, t) = 0$$

rather than the equation of continuity (see equation (2)), automatically embodying the condition that $J_z(0) = 0$. This underlies the incorrect conclusion drawn by Harris and others [14].

5.1. The positive-definiteness of γ_0

We substitute the expression of $\mathbf{E}(z)$ given by equations (17) and (18) into (26)–(30) and perform the integration over z' . We find it instructive to split $g(\mathbf{v}, z)$ into two parts, one denoted by $g_b(\mathbf{v}, z)$ and the other by $g_s(\mathbf{v}, z)$. They are given by

$$g_b(\mathbf{v}, z) = -ef'_0 \int_0^\infty dq \frac{4\rho_q}{K^2} (2F_+ \cos(qz) + 2iF_- \sin(qz) - \beta F_0 e^{-kz}), \quad (32)$$

where we have introduced the following functions,

$$F_\pm(\mathbf{K}, \bar{\omega}, \mathbf{v}) = \frac{1}{2} \left[\frac{\mathbf{K} \cdot \mathbf{v}}{\bar{\omega} - \mathbf{K} \cdot \mathbf{v}} \pm \frac{\mathbf{K} \cdot \mathbf{v}_-}{\bar{\omega} - \mathbf{K} \cdot \mathbf{v}_-} \right]. \quad (33)$$

Note that $F_{+/-}$ is an even/odd function of v_z . In addition,

$$F_0(\mathbf{k}, \bar{\omega}, \mathbf{v}) = \frac{\mathbf{k}^* \cdot \mathbf{v}}{\bar{\omega} - \mathbf{k}^* \cdot \mathbf{v}} = \sum_{l=1}^{\infty} \left(\frac{\mathbf{k}^* \cdot \mathbf{v}}{\bar{\omega}} \right)^l, \quad \mathbf{k}^* = (k, 0, ik). \quad (34)$$

Moreover, we have

$$g_s(\mathbf{v}, z) = \Theta(v_z) (-ef'_0) e^{i\frac{\bar{\omega}z}{v_z}} \int_0^\infty dq \frac{4\rho_q}{K^2} [\beta F_0(\mathbf{k}, \bar{\omega}, \mathbf{v}) - p\beta F_0(\mathbf{k}, \bar{\omega}, \mathbf{v}_-) + 2(p-1)F_+(\mathbf{K}, \bar{\omega}, \mathbf{v})]. \quad (35)$$

One may show that $g_b(\mathbf{v}, z)$ can also be obtained directly by Boltzmann's equation for an infinite system. Thus, this part contains exactly the responses of an infinite system. It is independent of surface properties, i.e. showing no dependence on the *Fuchs* parameter p , and the electrons incident on the surface (i.e. with $v_z < 0$) and those departing it (i.e. with $v_z > 0$) appear on equal footing in its expression.

On the other hand, $g_s(\mathbf{v}, z)$ signifies pure surface effects: it exists only for departing electrons, as indicated by the Heaviside function $\Theta(v_z)$ in its expression, and it depends on p thus reflecting on surface roughness. If we keep only $g_b(\mathbf{v}, z)$, the SRM will be revisited, making it evident that the SRM does not correspond to the limit of $p = 1$ (specularly reflecting surface), in contrast with its nominal meaning.

Another important feature of $g_s(\mathbf{v}, z)$ lies in its dependence on z , i.e. $g_s(\mathbf{v}, z) \propto e^{i\bar{\omega}z/v_z} \propto e^{-\gamma_0 z/v_z}$, which implies that $\gamma_0 \geq 0$ in accord with causality (see also preceding remarks above equation (26)). Otherwise, it would diverge far away from the surface.

5.2. Ω and G in the SCM

The conduction current density is also written in two parts, $\mathbf{J}_c(z) = \mathbf{J}_b(z) + \mathbf{J}_s(z)$, where $\mathbf{J}_{b/s}(z)$ are defined via equation (31) with $g(\mathbf{v}, z)$ replaced by $g_{b/s}(\mathbf{v}, z)$. For small $kv_F/\bar{\omega}$, we may keep only the first term in the series of $F_0(\mathbf{k}, \bar{\omega}, \mathbf{v})$. It is then straightforward to show that

$$\mathbf{J}_b(z) = \sigma_{\text{DM}}(\omega) \mathbf{E}(z) + \mathbf{J}_{\text{SRM}}(z), \quad (36)$$

where $\mathbf{J}_{\text{SRM}}(z)$ is responsible for the extension made through the SRM beyond the DM. It is given by²

$$J_{\text{SRM},x}(z) = \int \mathcal{D}q \mathcal{D}^3\mathbf{v} v_x F'_+(\mathbf{K}, \bar{\omega}, \mathbf{v}) \cos(qz), \quad (37)$$

$$J_{\text{SRM},z}(z) = i \int \mathcal{D}q \mathcal{D}^3\mathbf{v} v_z F'_-(\mathbf{K}, \bar{\omega}, \mathbf{v}) \sin(qz), \quad (38)$$

where we have defined a short-hand

$$\int \mathcal{D}q \mathcal{D}^3\mathbf{v} \dots = \left(\frac{m}{2\pi\hbar} \right)^3 \int_0^\infty dq \frac{4\rho_q}{K^2} \int d^3\mathbf{v} (-e^2 f'_0) \dots$$

together with these functions

$$F'_\pm(\mathbf{K}, \bar{\omega}, \mathbf{v}) = \frac{1}{2} \left[\frac{(\mathbf{K} \cdot \mathbf{v})^2}{1 - \mathbf{K} \cdot \mathbf{v}/\bar{\omega}} \pm \frac{(\mathbf{K} \cdot \mathbf{v}_-)^2}{1 - \mathbf{K} \cdot \mathbf{v}_-/\bar{\omega}} \right].$$

See that $J_{\text{SRM},z}(0) \equiv 0$, which makes no contribution to G . Now the total current density becomes

$$\mathbf{J}(z) = \mathbf{J}_b(z) + \mathbf{J}_s(z) + \mathbf{J}_p(z).$$

By definitions (6) and (11), we find

$$\Omega^2(K, \omega) = \Omega_0^2(\omega) + \frac{4\pi\bar{\omega}\mathbf{K} \cdot \mathbf{F}(\mathbf{K}, \bar{\omega})}{K^2}, \quad (39)$$

² In [10, 11], \mathbf{J}_{SRM} was called \mathbf{J}' . The expressions given there were typographically flawed, which though does not affect any statements or other expressions given in those work.

where \mathbf{F} is an odd function of $\bar{\omega}$ and given by

$$\mathbf{F}(\mathbf{K}, \bar{\omega}) = \left(\frac{m}{2\pi\hbar}\right)^3 \int d^3\mathbf{v} (-e^2 f'_0) \mathbf{v} \frac{(\mathbf{K} \cdot \mathbf{v}/\bar{\omega})^2}{1 - \mathbf{K} \cdot \mathbf{v}/\bar{\omega}}. \quad (40)$$

Partially performing the integral, we obtain

$$\Omega^2(K, \omega) = \omega_p^2 \left(1 - \frac{\bar{\omega}^2 \epsilon_p}{\omega_p^2} + \frac{3}{2} \frac{K v_F}{\bar{\omega}} \int_{-1}^1 dr \frac{r^3}{1 - r K v_F / \bar{\omega}} \right). \quad (41)$$

The real part of this expression approximates $\omega_p^2 \left(1 + \frac{3}{5} K^2 / k_p^2 \right)$ in the long wavelength limit, corresponding to the HDM limit with $v_0 = \sqrt{3/5} v_F$. Here $k_p = \omega_p / v_F$.

Landau damping. Obviously, the second term in equation (39) generally contains an imaginary part even in the collisionless limit where τ^{-1} is vanishingly small, due to a pole at $\bar{\omega} = \mathbf{K} \cdot \mathbf{v}$ in the integrand of the integral in \mathbf{F} . This part gives rise to Landau damping. For $\gamma_0 / \omega_p \ll 1$, we find for $\bar{\omega} = \omega_s + i\gamma_0$

$$\Omega^2(K, \omega) \approx \Omega_0^2 + \frac{3\omega_p^2 \mathcal{P}}{2} \int_{-1}^1 dr \frac{r^3}{\omega_s / K v_F - r} - i \frac{3\pi\omega_p^2}{2} \left(\frac{\omega_s}{K v_F} \right)^3 \Theta(K v_F - \omega_s). \quad (42)$$

Here \mathcal{P} takes the principal value. The sign of the second line depends on the sign of γ_0 . Only for $\gamma_0 > 0$, it is negative leading to damping, in line with causality. Equation (42) shows that, for bulk waves Landau damping exists only for sufficiently large K . For SPWs, however, Landau damping always exists, because q runs over all positive values in the secular equation (13).

A major improvement of the SCM over the SRM comes through the quantity $G(\mathbf{K}, \omega)$. In the SRM and its descendants, $G = G_0$ contains no symmetry breaking effects. In the SCM, one finds $G = G_0 + G_s$, where G_s stems from $J_s(0)$ and is given by

$$G_s(\mathbf{K}, \omega) = 4i\bar{\omega} \left(\frac{m}{2\pi\hbar} \right)^3 \int_{>} d^3\mathbf{v} v_z (-e^2 f'_0) [\beta F_0(\mathbf{k}, \bar{\omega}, \mathbf{v}) - p\beta F_0(\mathbf{k}, \bar{\omega}, \mathbf{v}_-) + 2(p-1)F_+(\mathbf{K}, \bar{\omega}, \mathbf{v})], \quad (43)$$

where ' $>$ ' indicates that the integral is restricted to departing electrons, i.e. $v_z \geq 0$. Note that G_s depends linearly on p .

5.3. The frequency and losses of SPWs

With Ω and G , we now proceed to solve equation (13) to find the frequency ω_s and damping rate γ of SPWs in the SCM.

Analytical analysis. As said before, the most significant improvement of the SCM over the SRM is through the term G_s . We wish to do an approximate analysis to explicitly demonstrate how $G_s = G'_s + iG''_s$ affects ω_s and γ .

For this purpose, let us write $G = G' + iG''$ and $\Omega = \Omega' + i\Omega''$ as well as $\epsilon = \epsilon' + i\epsilon''$, and assume that γ_0 / ω_s , G'' / G' and Ω'' / Ω' are all small quantities. Then, one can show that the real part of equation (13) gives

$$1 + \frac{1}{\omega_s^2} \int_0^\infty \frac{dq}{K^2} \frac{G'(\mathbf{K}, \omega_s)}{\epsilon'(\mathbf{K}, \omega_s)} \approx 0, \quad (44)$$

which determines the SPW frequency ω_s . The imaginary part of equation (13) yields γ_0 as

$$\gamma_0 \approx \omega_s (\eta_s - \eta_0), \quad (45)$$

where the contribution

$$\eta_s = \frac{1}{2} \int_0^\infty \frac{dq}{K^2} \frac{G''(\mathbf{K}, \omega_s)}{\epsilon'(\mathbf{K}, \omega_s)} \Big/ \int_0^\infty \frac{dq}{K^2} \frac{G'(\mathbf{K}, \omega_s)}{\epsilon'^2(\mathbf{K}, \omega_s)} \quad (46)$$

stems directly from the imaginary part G'' —which equals G''_s —of G , and

$$\eta_0 = \frac{\int_0^\infty \frac{dq}{K^2} \frac{G'(\mathbf{K}, \omega_s)}{\epsilon'(\mathbf{K}, \omega_s)} \frac{\Omega''(\mathbf{K}, \omega) \epsilon'(\mathbf{K}, \omega_s) - 1}{\Omega'(\mathbf{K}, \omega) \epsilon'(\mathbf{K}, \omega_s)}}{\int_0^\infty \frac{dq}{K^2} \frac{G'(\mathbf{K}, \omega_s)}{\epsilon'^2(\mathbf{K}, \omega_s)}} \quad (47)$$

comes directly from the imaginary part Ω'' of Ω . For stable systems, η_0 must be non-negative.

Note that Ω'' signifies Landau damping and inter-band absorption, as is clear from equation (42). As such, we may further split $\eta_0 = \eta_{\text{Landau}} + \eta_{\text{interband}}$, so that the SPW damping rate becomes

$$\gamma \approx \tau^{-1} + \gamma_{\text{Landau}} + \gamma_{\text{interband}} - \gamma_s, \quad (48)$$

where $\gamma_{\text{Landau, interband}, s} = \omega_s \eta_{\text{Landau, interband}, s}$, the first term represents Joule heating, the second and the third stand for Landau damping and inter-band absorption, respectively, while the last one is completely new due to $G'' = G''_s$. For models where $G_s = 0$, e.g. the DM, the HDM and the SRM, this new term is absent.

For the SCM, however, G_s is finite. Retaining only the first term in the series of F_0 , we find

$$G_s \approx -\frac{(1+p)\beta k \omega_p^2}{2\pi} + 8i\bar{\omega}(p-1)\left(\frac{m}{2\pi\hbar}\right)^3 \int_{>} d^3\mathbf{v} v_z (-e^2 f'_0) F_+(\mathbf{K}, \bar{\omega}, \mathbf{v}).$$

The second line here approximately corresponds to iG''_s . In general $G''_s \leq 0$ and hence $\eta_s \geq 0$. This implies that symmetry breaking effects tend to counteract the conventional damping and destabilize the metal. Our numerical solutions shall demonstrate that γ_0 is non-negative, in accord with the general argument given in section 5.1.

In the long wavelength limit $k \sim 0$, one has $k/K^2 \approx \pi\delta(q)$. Under this approximation, equation (44) becomes

$$\epsilon'(K_0, \omega_s) + \frac{\pi G'(K_0, \omega_s)}{2k\omega_s^2} \approx 0. \quad (49)$$

Here $\mathbf{K}_0 = (\mathbf{k}, 0)$. For models with $G_s = 0$, one immediately recovers from this equation the relation that $\epsilon_d + \epsilon' = 0$ as expected. For the SCM, however, one finds instead

$$\epsilon' + \epsilon_d \left(1 - \frac{1+p}{2} \frac{\omega_p^2}{\omega_s^2}\right) = 0. \quad (50)$$

This leads to

$$\omega_s \approx \omega_p \left(\frac{1 + \epsilon_d(1+p)/2}{1 + \epsilon_{pr} + \epsilon_d}\right)^{1/2}. \quad (51)$$

This result differs considerably from what is expected of other models. It shows that the value of the SPW frequency depends on surface conditions.

If we replace in equation (46) $\epsilon'(K, \omega_s)$ with its non-dispersive part, as is reasonable for small k , then we find

$$\eta_s \approx -\frac{1}{2\omega_p^2} \frac{1 + \epsilon_d}{1 + \epsilon_d(1+p)/2} \int_0^\infty dq \frac{G''_s(\mathbf{K}, \omega_s)}{K^2}, \quad (52)$$

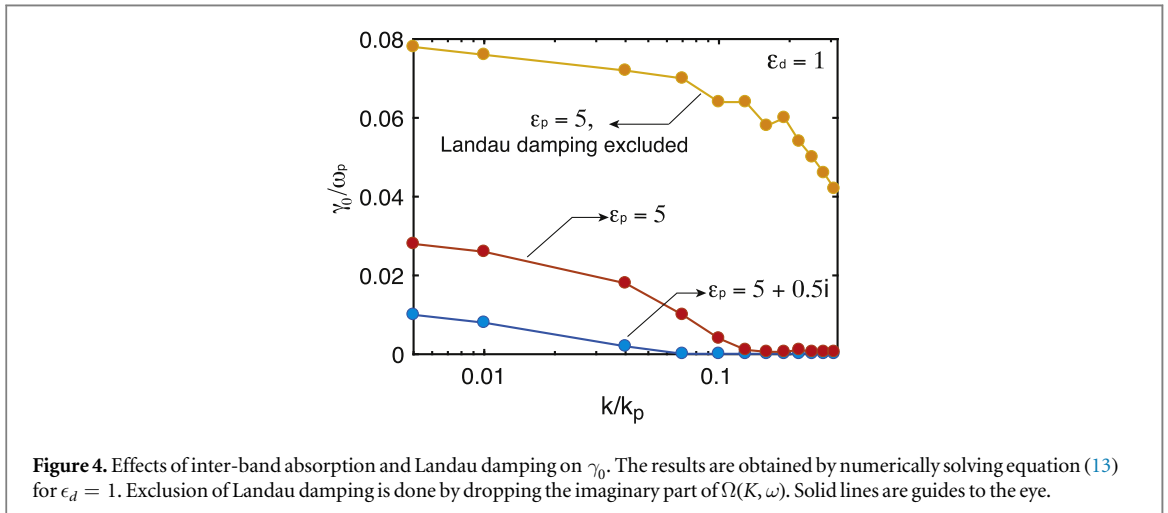
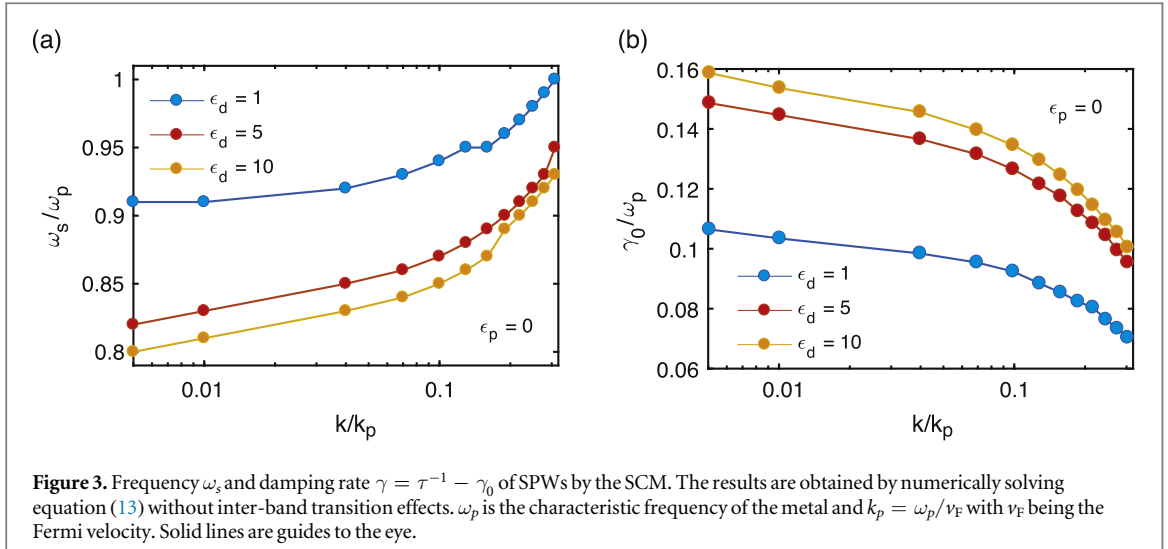
which implies that inter-band transitions have little effect on η_s , whereas a dielectric can enhance it by as much as 200%. This is to be borne out in numerical analysis in what follows.

Numerical analysis. We solve equation (13) numerically to find ω_s and γ_0 and how they vary with k and ϵ_d . We present the results for diffuse surfaces with $p = 0$ only. In equation (13), the integral over q extends to infinity. In numerical calculations, we impose a cutoff q_c . Roughly, $q_c \sim a^{-1}$, where a is a lattice constant. For metals, this means $q_c \sim k_F \sim k_p$. In all the numerical results presented here, we have chosen $q_c = 1.5k_p$. For q_c beyond this value, both ω_s and γ_0 quickly converge, confirming that the results are independent of the choice of q_c ³. Our results should be taken with a grain of salt for very small $k \ll \omega_s/c \approx k_p v_F/c \sim 0.01k_p$, where c is the speed of light in vacuum, because of retardation effects neglected in our theory.

The results are displayed in figures 3 and 4. In figure 3, we show $\bar{\omega} = \omega_s + i\gamma_0$ as a function of k for various ϵ_d but without inter-band transition effects ($\epsilon_p = 0$). As seen in figure 3(a), in agreement with the analytical expression of ω_s , increasing ϵ_d leads to smaller ω_s . Note that ω_s is considerably larger than what would be obtained by other models due to surface effects. Meanwhile, γ_0 increases with increasing ϵ_d , as seen in figure 3(b), in accord with equation (52). This increase comes from the factor β , i.e. the presence of a dielectric enhances the electric field at the surface; see equations (17) and (18).

The effects of inter-band absorption and Landau damping are illustrated in figure 4. Here we plot γ_0 for $\epsilon_d = 1$ under several circumstances as described in the figure. We see that inter-band transitions can strongly diminish γ_0 in two ways, as can be deduced from equations (51) and (52). Firstly, there is the screening effect (the curve with $\epsilon_p = 5$). This leads to smaller ω_s and hence smaller γ_0 , while leaving η_0 unaffected. Secondly, inter-band absorption further reduces γ_0 (see the curve with $\epsilon_p = 5 + 0.5i$). As for Landau damping, it is sizable and generally increases with k ; see [5, 12]. As such, γ_0 decreases as k increases. In relation to this feature, we should mention a size effect [11]: in films of thickness d , γ_0 is strongly suppressed and quickly diminishes to zero when the wavelength becomes longer than d . Echoing this, one can show that $\gamma_0 \sim kv_F$ vanishes for $k \sim 0$ in the SIM [46].

³ The solutions to equation (13) are independent of the choice of q_c as long as the latter is sufficiently large. For example, for $k = 0.07k_p$, we find that $\bar{\omega}/\omega_p = 0.93 + 0.095i, 0.95 + 0.099i, 0.95 + 0.099i, 0.96 + 0.098i$ for $q_c/k_p = 1.5, 3.0, 4.5, 6.0$, respectively. There is no difference within the numerical resolution ± 0.005 . More discussions on this can be found in [46].



6. Possible lossless SPWs by the SCM

According to the SCM, the SPW loss rate is $\gamma = \tau^{-1} - \gamma_0$. In view of energy conversion, the expression implies a competition between the loss due to thermalization and the gain due to energy transferred from the electrons to the waves [12]. Should the condition $\gamma_0\tau = 1$ be fulfilled, lossless SPWs may be produced. In this section, we discuss this possibility against two common plasmonic metals: silver and aluminum.

Note that τ^{-1} is the collision rate at the SPW frequency ω_s . Even at zero temperature and in defect-free samples, there is sufficient phase space—available due to the effective temperature $\hbar\omega_s/k_B$ —for electronic scattering and thus τ^{-1} is comparable to ω_p . Up to our knowledge, there is virtually no direct data on τ^{-1} for any materials. We then opt to estimate it by the following formula [32],

$$\tau^{-1} \approx \gamma_{\text{residual}} + 4\nu_0 \left(\frac{T}{T_D} \right)^5 \int_0^{T_D/T} \frac{y^4 dy}{e^y - 1} + \omega_p \left(\frac{k_B T}{\hbar\omega_p} \right)^2, \quad (53)$$

where γ_{residual} is the residual rate given by

$$\gamma_{\text{residual}} \approx \frac{2\nu_0}{5} + \frac{\omega_p}{4\pi^2} \left(\frac{\omega_s}{\omega_p} \right)^2 + \gamma_{\text{impurity}}. \quad (54)$$

Here the first contribution comes from phonon scattering, the second from electron–electron scattering and the third due to impurity scattering to be neglected hereafter. The second term generally underestimates the electron–electron rate in noble metals and Al by a few times [53]⁴. The coefficient $\nu_0 \sim k_B T_D/\hbar$ may be

⁴ More detailed calculations [53] shows that the second term in equation (54) should be multiplied by a factor $(\pi^3/12)\Gamma\Delta(\hbar\omega_p/\epsilon_F)$ where Γ and Δ are constants with their product of the order of 0.4—for noble metals and Al [62]—related to the geometry of the Fermi surface. Similarly, the third term in equation (53) should be multiplied by the same factor. For noble metals and Al this factor is around 1.5. However, for sodium and potassium it is nearly zero.

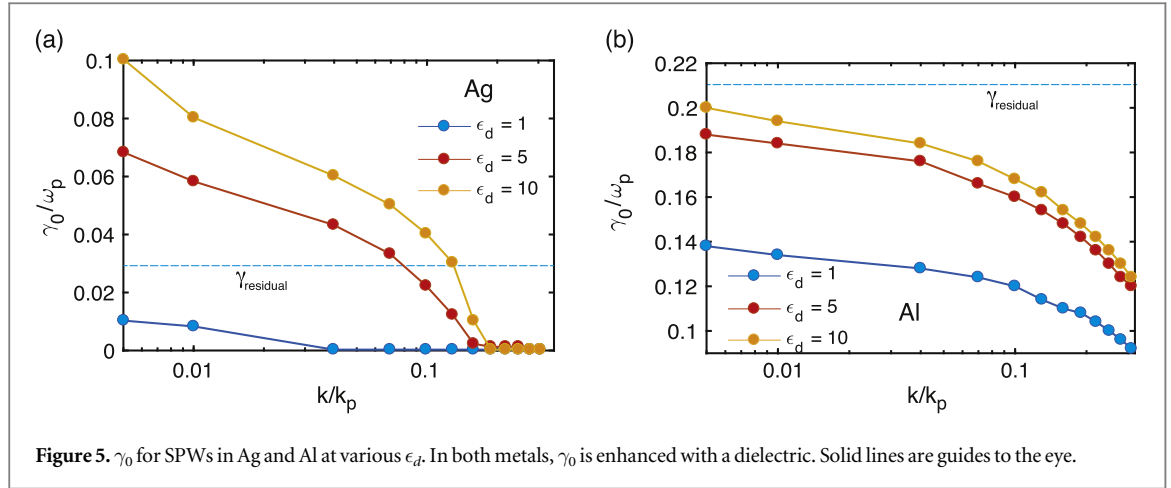


Figure 5. γ_0 for SPWs in Ag and Al at various ϵ_d . In both metals, γ_0 is enhanced with a dielectric. Solid lines are guides to the eye.

determined from the slope of the phononic part of the D.C. conductivity at temperatures higher than the Debye temperature T_D . Equation (54) shows that γ_{residual} may well amount to quite a few percentages of ω_p for metals.

Silver. In silver electronic transitions involving the 5s and 4d bands have a dramatic effect on the properties of SPWs [35, 54, 55], leading to $\hbar\omega_s \approx 3.69$ eV and $\hbar\omega_b \approx 3.92$ eV at long wavelengths, both lying far below the characteristic frequency $\hbar\omega_p = 9.48$ eV. Experimentally [32, 56], it was found that $\hbar\nu_0 \sim 0.1\text{eV} \sim 0.01\hbar\omega_p$, in consistency with the value of $T_D \approx 220$ K for Ag. The electron–electron scattering rate according to equation (54) would be less than one percent of ω_p , while experimental measurements and more accurate expressions [53] place it about $0.02\omega_p$. As such, we may reasonably take $\gamma_{\text{residual}} \sim 0.03\omega_p$ as an estimate.

The damping rate γ can be read out from the line shape of the electron energy loss spectra (EELS). The temperature dependence of γ has been recorded on a high-quality Ag single crystal by means of EELS [57, 58]. The data indicates that at low temperature γ amounts to less than one percent of ω_p , a value a few times smaller than the as-projected γ_{residual} . If Landau damping and inter-band absorption are also counted, the discrepancy can be more dramatic. In light of the present theory, this discrepancy gives an estimate of γ_0 . The values suggest that γ_0 has substantially compensated for the collision losses, i.e. $\gamma_0 \sim \gamma_{\text{residual}}$, as borne out in the following analysis.

To evaluate γ_0 , $\epsilon_p(\omega)$ needs to be supplied. Combining a semi-quantum model and ellipsometry as well as transmittance-reflectance measurements, Rakić *et al* [36] employed K–K analysis and prescribed a parametrized dielectric function— $\hat{\epsilon}_r^{(b)}(\omega)$ in their notation—for the inter-band contribution. Here, we use their fitting as an input for $\epsilon_p(\omega)$ but with a number of caveats. Firstly, their dielectric function was deduced from measurements assuming the conventional electromagnetic responses without any surface effects considered in the present paper. These effects, however, should be considered when analyzing ellipsometry and reflectance spectra. A future study will be made to address this issue. Secondly, their function very poorly reproduces the electron energy loss spectra and the reflectance spectra, especially near the SPW frequency of interest. Thirdly, their function does not give an accurate partition into inter-band and intra-band contributions, e.g. $\omega_p \approx 8$ eV was used rather than the widely agreed 9.48 eV [55], which may overestimate the inter-band transition effects. Finally, their function is defined only for real frequency, and thus in general not suitable for $\epsilon_p(\omega)$, where ω is complex. To remedy this point, we substitute $\hat{\epsilon}_r^{(b)}[\text{Re}(\omega)]$ for $\epsilon_p(\omega)$, which should be reasonable if $\gamma/\omega_s \ll 1$.

The results are displayed in figure 5(a), where the computed γ_0 is exhibited as a function of k at various values of ϵ_d . While γ_0 for SPWs supported on a pristine Ag surface (i.e. $\epsilon_d = 1$) is negligibly small and way below γ_{residual} , by using a dielectric it can be significantly enhanced at long wavelengths beyond γ_{residual} . This trend is consistent with equation (52). The fact that γ_0 can be made higher than γ_{residual} suggests the possibility of compensating for the plasmonic losses completely in Ag. The situation is shown in figure 6. By interfacing the metal with a lossless dielectric of $\epsilon_d = 5$ and cooling it down toward a critical temperature $T^* \sim 120$ K, one can diminish the net losses as much as desired. It should be mentioned that, ϵ_d is the constant at the frequency ω_s as well.

Aluminum. Inter-band transitions in Al are widely considered less pronounced than in Ag. Nevertheless, their presence can still be felt, e.g. in the difference between the values of $\hbar\omega_p \approx 12.6$ eV and $\hbar\omega_b \approx 15.3$ eV. These numbers were obtained by density functional theory [59] and experimental fitting [37]. In addition, $\hbar\omega_s \approx 10.7$ eV [60, 61]. γ_{residual} may be deduced from the experimental measurements performed by Sinvani *et al* [62] and others [63]. These authors measured the low temperature dependence of the d.c. resistivity ρ of Al. Their data shows that $\rho \approx \rho_0 + AT^2 + B(T/T_D)^5$, where ρ_0 stems from impurity and lattice dislocation scattering while A and B are constants characterizing electron–electron scattering and electron–phonon scattering, respectively. Analyzing the data, the authors found that $A \approx 0.21$ p Ω cm K^{−2} (a lower bound) and

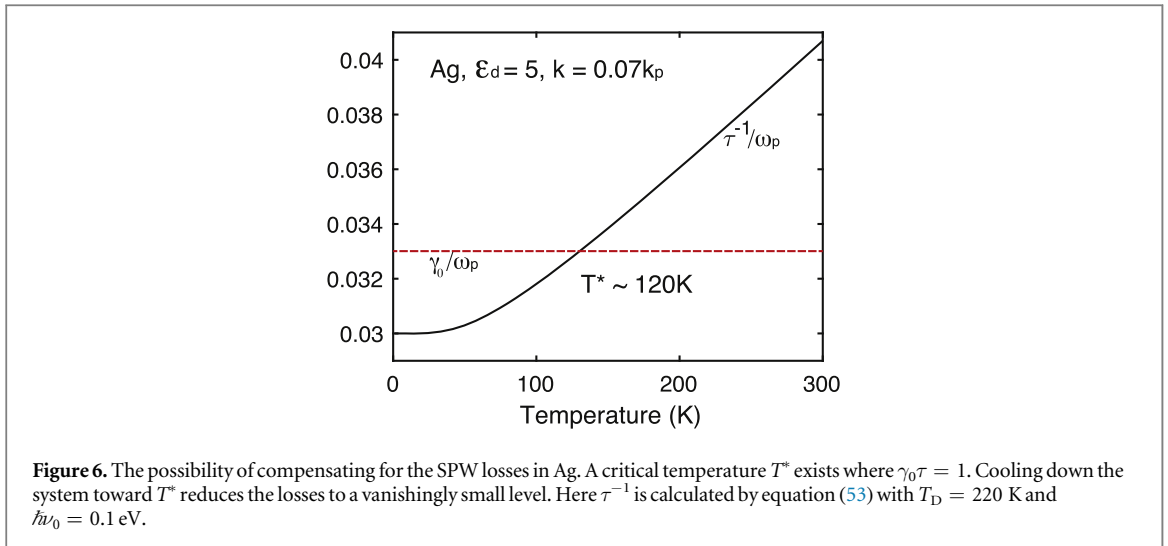


Figure 6. The possibility of compensating for the SPW losses in Ag. A critical temperature T^* exists where $\gamma_0\tau = 1$. Cooling down the system toward T^* reduces the losses to a vanishingly small level. Here τ^{-1} is calculated by equation (53) with $T_D = 220$ K and $\hbar\nu_0 = 0.1$ eV.

$B \approx 4.9 \times 10^4 \mu\Omega$ cm for $T_D = 430$ K. From this we obtain $\nu_0 \approx 0.18\omega_p$ and the residual electron–electron scattering rate—a few times larger than what would be obtained with equation (54) [32]—approximating $0.14\omega_p$, yielding $\gamma_{\text{residual}} \approx 0.21\omega_p$. It is noted that this value is comparable to the width (~ 1.5 eV, nearly $0.12\omega_p$) of the electron energy loss peak near the frequency of the bulk plasma waves in Al [60]. The as-obtained ν_0 (and hence γ_{residual}) represents probably an overestimate⁵.

To compute γ_0 , we again resort to the fitting function constructed by Rakić *et al* [37] and have it in place of $\epsilon_p(\omega)$ in our theory, in the same way as we did in the case of Ag. It goes without saying that the same caveats should be kept in mind. The results are shown in figure 5(b). As expected, γ_0 is comparable to that in the absence of inter-band transitions (see figure 3(b)), as these transitions are weak in Al. As is with Ag, γ_0 of SPWs in Al can also be fortified—but to a lesser extent—by a dielectric. Nevertheless, the enhanced γ_0 still falls short of γ_{residual} unless for very long wavelengths where retardation effects need to be properly accounted for.

The calculations reported in the above have assumed $p = 0$. For surfaces strongly reflecting electrons (i.e. $p > 0$), γ_0 could be much lower [12]. We also point out that additional losses such as due to SPWs converted into radiation are not considered. They can be absorbed in the definition of τ^{-1} .

7. Conclusions

In order to answer the two questions posed at the beginning of this paper, i.e. (i) why had not previous work hit at the possibility of lossless SPWs and (ii) how far is the latter from reality, we have derived a universal macroscopic theory of SPWs that applies to any electron dynamics. In light of the theory, our answer to question (i) is simple: lossless waves are possible only within a self-consistent description of physical surfaces that takes care of translation symmetry breaking effects, a condition not met in existing work. As for question (ii), we can only suggest an optimistic prospect rather than an answer due to various uncertainties in inter-band transition effects: our estimate shows that lossless waves may well be within the reach in some materials.

Our results reveal two contradictory views regarding SPW losses, as compared in table 1. According to the conventional framework, as exemplified by the DM, the HDM and the SRM,

$$\gamma^{(1)} = \tau^{-1} + \gamma_{\text{Landau}} + \gamma_{\text{interband}}$$

and thus the SPW loss rate cannot be smaller than either of τ^{-1} and γ_{Landau} . On the other hand, within the SCM, a totally different picture emerges, giving

$$\gamma^{(2)} = \tau^{-1} - \gamma_0, \quad \gamma_0 = \gamma_s - \gamma_{\text{Landau}} - \gamma_{\text{interband}}$$

which suggests that the loss rate is always smaller than τ^{-1} . Here $\gamma_s = \eta_0\omega_s$, see equation (51). To directly contrast these two views, one has to measure separately τ^{-1} and γ . While the latter can be measured in many ways, the former is difficult to be directly measured. In what follows, we mention some indirect observations defying $\gamma^{(1)}$ but supporting $\gamma^{(2)}$.

⁵ The often quoted resistivity for Al at room temperature is around $3 \mu\Omega$ cm, see [70]. Using this to evaluate the contribution of the electron–phonon scattering to τ^{-1} would give $\nu_0 \approx 0.01\omega_p$, a much smaller value than what would be obtained with the low temperature data in [62, 63]. This discrepancy might be due to the uncertainty as to the actual scattering mechanism responsible for the resistivity at low temperatures.

Firstly, we note that $\gamma^{(2)}$ naturally resolves a long-standing puzzle, that of the apparent insignificance of Landau damping even at very short wavelengths [38]. For example, in single crystal Ag, the loss rate measured by EELS [57, 58] is $\sim 1\%\omega_p$ even for $k \sim 1 \text{ nm}^{-1}$, whereas $\gamma_{\text{Landau}} \sim kv_F \sim 10\%\omega_p$. This discrepancy is inexplicable by $\gamma^{(1)}$, but easily comprehensible by $\gamma^{(2)}$, i.e. Landau damping has been overcompensated by γ_s .

Secondly, we note that the loss rate of bulk plasma waves differs from that of SPWs primarily because of the absence of γ_0 in the former, as least in materials where inter-band effects are not important. In those materials, bulk waves should be generally much more lossy than SPWs, an observation that seems in consistency with experience. For example [64], the loss rates for the SPWs and the bulk waves in potassium are $0.1\text{eV}\hbar^{-1}$ and $0.24\text{eV}\hbar^{-1}$, respectively, while those in cesium are $0.23\text{eV}\hbar^{-1}$ and $0.75\text{eV}\hbar^{-1}$, respectively. In spite of these, the general situation is obviously unclear at this stage.

Finally, we mention an experiment performed on a van der Waals structure by Iranzo *et al* [65]. These authors were able to confine propagating plasmon between a graphene layer and a metal array to the atomic limit without sacrificing its lifetime, which obviously beats the limit set by Landau damping. From an energy conversion point of view [12], the plasmon in such a structure is not much different from the surface plasmon on a metal surface. Their result is compatible with $\gamma^{(2)}$: in ultimate confinement γ_0 tends to zero due to increase of Landau damping (figure 4), leaving the loss rate saturating at τ^{-1} , as observed. We anticipate a similar trend for the losses of local plasmon resonance on metal particles.

In the SCM we have assumed that the ground state of the underlying metal be simply the Fermi sea. The fact that γ can be made negative means an instability of the Fermi sea. Upon entering such circumstances, the metals are expected to undergo a transition into a different stable state, of which the electrical responses cannot be captured by our current SCM calculations. We will clarify the nature of this transition in the future.

The results reported in this work should be of broad interest to the researchers working in plasmonics, surface science and condensed matter physics. We hope that experimentalists will find the results fascinating enough to put their hands on them.

Acknowledgments

The author enjoyed the hospitality during his stay with K Wakabayashi's group at Kwansai Gakuin University, Japan, where part of the writing was undertaken. This work is not supported by any funding bodies.

Appendix A. SPWs in the HDM

Here we show that the usually claimed SPWs in the HDM are incompatible with the waves in the DM. We put $\epsilon_p = 0$ and $\epsilon_d = 1$ for simplicity. In the HDM, the electrons are treated as a fluid described by two field quantities: the velocity field $\mathbf{v}(\mathbf{x}, t)$ and the electron density field $n_0 + n(\mathbf{x}, t)$, where $n(\mathbf{x}, t)$ denotes the deviation from the mean density n_0 . The charge density is then $\rho(\mathbf{x}, t) = n(\mathbf{x}, t)e$ and the current density is $\mathbf{J}(\mathbf{x}, t) = e(n_0 + n(\mathbf{x}, t))\mathbf{v}(\mathbf{x}, t)$, which in the linear responses regime becomes $\mathbf{J}(\mathbf{x}, t) = n_0 e\mathbf{v}(\mathbf{x}, t)$.

A small fluid element of volume δV feels a force consisting of two portions: the electric force $n_0 e\delta V \mathbf{E}(\mathbf{x}, t)$ and the pressure due to density variation $-m\delta V v_0^2 \partial_x n(\mathbf{x}, t)$. Now the laws of mechanics states that in the linear regime one has

$$n_0 m \left(\partial_t + \frac{1}{\tau} \right) \mathbf{v}(\mathbf{x}, t) = n_0 e \mathbf{E}(\mathbf{x}, t) - m v_0^2 \partial_x n(\mathbf{x}, t), \quad (\text{A1})$$

Here shear viscosity effects have been ignored. Now assuming $n(\mathbf{x}, t) = n(\mathbf{x}) e^{-i\omega t}$ and similarly for $\mathbf{v}(\mathbf{x}, t)$ and other field quantities, we obtain the current density as

$$\mathbf{J}(\mathbf{x}) = \frac{i}{\omega} \left(\frac{\omega_p^2}{4\pi} \mathbf{E}(\mathbf{x}) - v_0^2 \partial_x \rho(\mathbf{x}) \right), \quad (\text{A2})$$

the divergence of which is then given by

$$\partial_x \cdot \mathbf{J}(\mathbf{x}) = \frac{i}{\omega} (\omega_p^2 - v_0^2 \partial^2) \rho(\mathbf{x}). \quad (\text{A3})$$

Combining this equation with the equation of continuity, one obtains the wave equation for the charge density.

The usually quoted SPWs. In the standard but erroneous prescription for SPWs in this model, one takes $J_z(\mathbf{x}_0) \equiv 0$, or equivalently

$$v_z(\mathbf{x}_0) \equiv 0. \quad (\text{A4})$$

Here \mathbf{x}_0 denotes a point on the surface. The continuity equation reads

$$-i\bar{\omega}\rho(\mathbf{x}) + \partial_{\mathbf{x}} \cdot \mathbf{J}(\mathbf{x}) = 0. \quad (\text{A5})$$

In conjunction with equation (A3), one finds

$$(\omega_p^2 - \bar{\omega}^2 - v_0^2 \partial^2) \rho(\mathbf{x}) = 0, \quad (\text{A6})$$

which is equation (23) given in section 2.3. One then seeks solutions of the form $\rho(\mathbf{x}) = \rho(z)e^{ikx}$ and similarly for other quantities. Further, taking $\rho(z) = \rho_0 e^{-\kappa z}$ and substituting it in equation (A6), we obtain

$$\omega_p^2 + v_0^2(k^2 - \kappa^2) - \bar{\omega}^2 = 0. \quad (\text{A7})$$

The boundary condition (A4) requires

$$\frac{\omega_p^2}{4\pi} E_z(0) = v_0^2 \rho'(0) = -\kappa v_0^2 \rho_0, \quad \rho'(z) = \partial_z \rho(z). \quad (\text{A8})$$

It is easy to show that

$$E_z(0) = -\frac{2\pi\rho_0}{k + \kappa}.$$

With this it follows from equation (A8) that

$$\omega_0^2 = v_0^2 \kappa(k + \kappa), \quad \omega_0 = \omega_p / \sqrt{2}. \quad (\text{A9})$$

Combining this relation with equation (A6), we arrive at

$$\bar{\omega}^2 = \omega_0^2 + \omega_0 v_0 k. \quad (\text{A10})$$

This is the usually quoted dispersion relation claimed for the SPWs in the HDM. As briefly captured in section 2.3, this claim is plainly false: in the limit $v_0 \rightarrow 0$, $\kappa \sim v_0^{-1}$ diverges and hence $\int_0^\infty dz \rho(z) = \rho_0 \kappa^{-1} \sim \rho_0 v_0$ vanishes, thus in contradiction with the DM. This would also erroneously imply that $E_z(z)$ did not change sign across the surface charge layer. It was essentially this erroneous solution that had been identified by Harris [14] and Garcia *et al* [15] in their study based on Boltzmann's equation. It is plausible that this is also so with works employing a more microscopic approach such as the density functional theory, at least those using the so-called 'infinite barrier' model for mimicking the surface [30]. For example, Feibelman identified a solution of uniform potential and hence empty of charges but with frequency $\omega_p / \sqrt{2}$ in the long wavelength limit [47], exactly in this kind.

SPWs in the HDM by the present theory. In our theory, no restrictions are placed on $J_z(\mathbf{x}_0)$ and thus the equation of continuity reads

$$-i\bar{\omega}\rho(\mathbf{x}) + \partial_{\mathbf{x}} \cdot \mathbf{J}(\mathbf{x}) = -\Theta'(z)J_z(\mathbf{x}_0). \quad (\text{A11})$$

Using equation (A3) and taking $\rho(\mathbf{x}) = \rho(z)e^{ikx}$ and similarly for other quantities, one finds

$$(\omega_p^2 + v_0^2 k^2 - v_0^2 \partial_z^2 - \bar{\omega}^2) \rho(z) = i\bar{\omega}J_z(0)\Theta'(z). \quad (\text{A12})$$

Now we introduce the Fourier transform for

$$\rho(z) = (2/\pi) \int_0^\infty dq \rho_q \cos(qz).$$

It follows that

$$J_z(0) = (i/\bar{\omega})(\omega_p^2/4\pi)E_z(0) = \sigma_{\text{DM}}E_z(0).$$

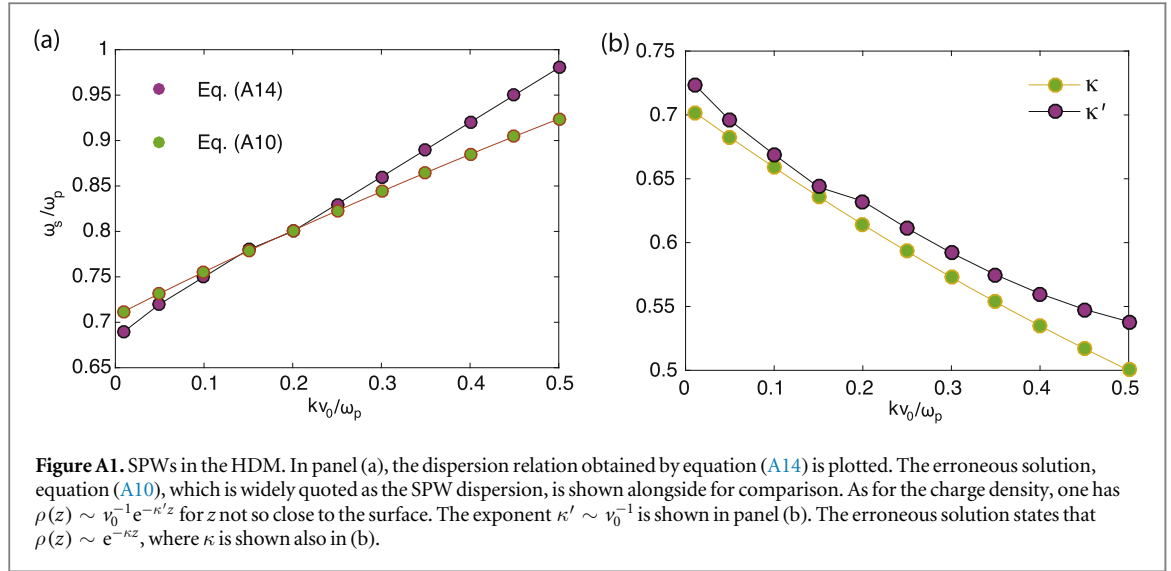
This implies that $\rho'(0) = 0$, which must hold for any $\rho(z)$ that reduces to the Dirac function $\delta(z)$ desired in the DM limit. In conjunction with

$$E_z(0) = -\int_0^\infty dq \frac{4k\rho_q}{K^2}, \quad (\text{A13})$$

we find from equation (A11) that

$$1 - \frac{\omega_p^2}{4\pi} \int_0^\infty dq \frac{k}{K^2} \frac{1}{\omega_p^2 + v_0^2 K^2 - \bar{\omega}^2} = 0, \quad (\text{A14})$$

which is just equation (21) displayed in section 2.3. The dispersion relation obtained by this equation has been plotted in figure A1(a), where the relation (A10) is displayed together for comparison. Both exhibit a linear dependence on k but with different slopes. Our theory predicts a slightly bigger slope.



Let us have a look at the profile of $\rho(z)$. According to our theory,

$$\rho(z) = i\bar{\omega}J_z(0) \int \frac{dq}{\pi/2} \cos(qz)(\omega_p^2 + v_0^2 K^2 - \bar{\omega}^2)^{-1}.$$

With $\tilde{q} = qv_0/\omega_p$ and $\tilde{K} = Kv_0/\omega_p$ as well as $\tilde{z} = zv_0/\omega_p$, it can be rewritten as

$$\rho(z) = \frac{i\bar{\omega}J_z(0)}{\omega_p v_0} \tilde{\rho}(z), \tag{A15}$$

where

$$\tilde{\rho}(z) = \int \frac{d\tilde{q}}{\pi/2} \cos(\tilde{q}\tilde{z})(1 + \tilde{K}^2 - (\bar{\omega}/\omega_p)^2)^{-1}. \tag{A16}$$

One can show that not so close to the surface $\tilde{\rho}(z) = \frac{1}{\kappa' v_0/\omega_p} e^{-\kappa' z}$, where

$$\kappa' = \frac{\omega_p}{v_0} \sqrt{1 + \tilde{k}^2 - (\bar{\omega}/\omega_p)^2}$$

with $\tilde{k} = kv_0/\omega_p$. Thus,

$$\int \rho(z) dz = \frac{i\bar{\omega}J_z(0)}{\omega_p^2} \frac{1}{1 + \tilde{k}^2 - (\bar{\omega}/\omega_p)^2}.$$

For $\tilde{k} = 0$, it reduces to that for the DM. The dependence of κ' on k is shown in figure A1(b), alongside that of κ .

Appendix B. Origin of SPWs in the SRM

The widely used SRM assumes that the electrons be specularly reflected off a surface. One would then expect that $J_z = 0$ and no SPWs would exist in this model. However, in the main text we have shown that what the SRM actually does is an extension of the HDM. The question then is, how do SPWs originate in the SRM? Here we show that the answer lies with the ‘fictitious’ charge sheet assumed in the model.

We follow the SRM formalism as explained in many papers [20, 26, 66–69] and employ it to study the response to an external distribution of charge $\rho_{\text{ext}}(z; \mathbf{k}, \omega)$ placed outside the metal. We take $\rho_{\text{ext}}(z; \mathbf{k}, \omega) = \rho_0(\mathbf{k}, \omega)\delta(z - z_0)$ for simplicity, where $z_0 < 0$. In the SRM, the total electrostatic potential, $\phi_{\text{tot}}(z; \mathbf{k}, \omega) = \phi(z; \mathbf{k}, \omega) + \phi_{\text{ext}}(z; \mathbf{k}, \omega)$, where ϕ is the potential produced by the induced charges $\rho(z; \mathbf{k}, \omega)$, is written

$$\phi_{\text{tot}}(z; \mathbf{k}, \omega) = \Theta(z)\phi_m(z; \mathbf{k}, \omega) + \Theta(-z)\phi_v(z; \mathbf{k}, \omega), \tag{B1}$$

where ϕ_m and ϕ_v are the potentials in the so-called pseudo-metal and pseudo-vacuum, respectively. These are further defined by

$$\phi_{m/v}(\mathbf{Q}, \omega) = \frac{4\pi}{Q^2 \epsilon_{m/v}(\mathbf{Q}, \omega)} [\rho_{\text{ext}}^{m/v}(\mathbf{Q}, \omega) + \sigma_s^{m/v}(\mathbf{k}, \omega)], \tag{B2}$$

where $\phi_{m/v}(\mathbf{Q}, \omega) = \int_{-\infty}^{\infty} dz e^{-iqz} \phi_{m/v}(z; \mathbf{k}, \omega)$ is the ordinary Fourier transform, $\mathbf{Q} = (\mathbf{k}, q)$, $\epsilon_m(\mathbf{Q}, \omega) = \epsilon(Q, \omega)$, $\epsilon_v(\mathbf{Q}, \omega) = 1$ and $\sigma_s^{m/v}(\mathbf{k}, \omega)$ is the fictitious surface charge density. In addition, $\rho_{\text{ext}}^{m/v}$ is related to ρ_{ext} as follows

$$\rho_{\text{ext}}^{m/v}(z; \mathbf{k}, \omega) = \Theta(z) \rho_{\text{ext}}(\mp z; \mathbf{k}, \omega) + \Theta(-z) \rho_{\text{ext}}(\pm z; \mathbf{k}, \omega). \quad (\text{B3})$$

It follows that $\rho_{\text{ext}}^v(\mathbf{Q}, \omega) = 0$ and

$$\rho_{\text{ext}}^m(\mathbf{Q}, \omega) = 2\rho_0(\mathbf{k}, \omega) \cos(qz_0). \quad (\text{B4})$$

Equations (B1)–(B3) define the SRM. Requiring the continuity of the dielectric displacement at $z = 0$ leads to

$$\sigma_s^m(\mathbf{k}, \omega) = -\sigma_s^v(\mathbf{k}, \omega) = \sigma_s(\mathbf{k}, \omega). \quad (\text{B5})$$

This can be further fixed by requiring the continuity of ϕ_{tot} at $z = 0$. One finds

$$\sigma_s(\mathbf{k}, \omega) = 2\rho_0(\mathbf{k}, \omega) \cosh(kz_0) \epsilon_{s,\text{SRM}}^{-1}(\mathbf{k}, \omega), \quad (\text{B6})$$

where $\epsilon_{s,\text{SRM}}$ is as given in section 4.3, i.e.

$$\epsilon_{s,\text{SRM}}(\mathbf{k}, \omega) = 1 + \frac{k}{\pi} \int_{-\infty}^{\infty} \frac{dq}{Q^2 \epsilon(Q, \omega)}.$$

The zeros of this quantity give poles of σ_s corresponding to SPWs in the SRM, thus revealing that the fictitious charge sheet is responsible for the SPWs in the SRM.

ORCID iDs

Hai-Yao Deng  <https://orcid.org/0000-0001-6065-483X>

References

- [1] Barnes W L, Dereux A and Ebbesen T W 2003 Surface plasmon subwavelength optics *Nature* **424** 828
- [2] Zayats A V, Igor I S and Maradudin A A 2005 Nano-optics of surface plasmon polaritons *Phys. Rep.* **408** 131
- [3] Maier S A 2007 *Plasmonics: Fundamentals and Applications* (New York: Springer)
- [4] Sarid D and Cgallener W 2010 *Modern Introduction to Surface Plasmons: Theory, Mathematic Modeling and Applications* (Cambridge: Cambridge University Press)
- [5] Khurgin J B and Boltasseva A 2012 Reflecting upon the losses in plasmonics and metamaterials *MRS Bull.* **37** 768
Khurgin J B and Boltasseva A 2015 How to deal with the loss in plasmonics and metamaterials *Nat. Nanotechnol.* **10** 2
Khurgin J B and Boltasseva A 2015 Ultimate limit of field confinement by surface plasmon polaritons *Faraday Discuss.* **178** 109
Khurgin J B and Boltasseva A 2012 How small can ‘Nano’ be in a ‘Nanolaser’? *Nanophotonics* **1** 3
- [6] Oulton R F 2012 Plasmonics: loss and gain *Nat. Photon.* **6** 219
Oulton R F 2012 Surface plasmon lasers: sources of nanoscopic light *Mater. Today* **15** 26
- [7] Stockman M I 2008 Spasers explained *Nat. Photon.* **2** 327
- [8] Hess O, Pendry J B, Maier S A, Oulton R F, Hamm J M and Tsakmakidis K L 2012 Active nanoplasmonic metamaterials *Nat. Mater.* **11** 573
- [9] Premaratne M and Stockman M I 2017 Theory and technology of SPASERs *Adv. Opt. Photonics* **31** 79–128
- [10] Deng H-Y, Wakabayashi K and Lam C-H 2017 universal self-amplification channel for surface plasma waves *Phys. Rev. B* **95** 045428
- [11] Deng H-Y 2017 Theory of nonretarded ballistic surface plasma waves in metal films *Phys. Rev. B* **95** 125442
- [12] Deng H-Y 2017 Possible instability of the Fermi sea against surface plasma oscillations *J. Phys. Condens. Matter* **29** 455002
- [13] Ritchie R H 1957 Plasma losses by fast electrons in thin films *Phys. Rev.* **106** 874
Stern E A and Ferrell R A 1960 Surface plasma oscillations of a degenerate electron gas *Phys. Rev.* **120** 130
- [14] Harris J 1972 The effect of short range correlations on surface plasmon dispersion *J. Phys. C: Solid State Phys.* **5** 1757
- [15] Flores F and Garcia-Moliner F 1977 Classical electrodynamics of non-specular conducting surfaces *J. Phys.* **38** 863
- [16] Ritchie R H 1963 On surface plasma oscillations in metal foils *Prog. Theor. Phys.* **29** 607
- [17] Harris J 1971 Surface plasmon dispersion: a comparison study of microscopic and hydrodynamics theories *Phys. Rev. B* **4** 1022
Nakamura Y O 1983 Quantization of non-radiative surface plasma oscillations *Prog. Theor. Phys.* **70** 908
- [18] Barton G 1979 Some surface effects in the hydrodynamic model of metals *Rep. Prog. Phys.* **42** 65
- [19] Fetter A L 1973 Electrodynamics of a layered electron gas: I. single layer *Ann. Phys.* **81** 367
Fetter A L 1986 Edge magnetoplasmons in a two-dimensional electron fluid confined to a half-plane *Phys. Rev. B* **33** 3717
- [20] Ritchie R H and Marusak A L 1966 The surface plasmon dispersion relation for an electron gas *Surf. Sci.* **4** 234
- [21] Nunez R, Echenique P M and Ritchie R H 1980 The energy loss of energetic ions moving near a solid surface *J. Phys. C: Solid State Phys.* **13** 4229
- [22] Vagov A, Larkin I A, Croitoru M D and Axt V M 2016 Role of nonlocality and Landau damping in the dynamics of a quantum dot coupled to surface plasmons *Phys. Rev. B* **93** 195414
- [23] Pekar S I 1958 The theory of electromagnetic waves in a crystal in which excitons are produced *Sov. Phys. JETP* **6** 785
- [24] Maradudin A A and Mills D L 1973 Effect of spatial dispersion on the properties of a semi-infinite dielectric *Phys. Rev. B* **7** 2787
- [25] Garcia-Moliner F and Flores F 1977 Classical electrodynamics of non-specular dielectric surfaces *J. Phys.* **38** 851
- [26] Flores F and Garcia-Moliner F 1979 Self-energy of a fast-moving charge near a surface *J. Phys. C: Solid State Phys.* **12** 907
- [27] Feibelman P J 1982 Surface electromagnetic fields *Prog. Surf. Sci.* **12** 287
- [28] Tsuei K-D, Plummer E W, Liebsch A, Pehlke E, Kempa K and Bakshi P 1991 The normal modes at the surface of simple metals *Surf. Sci.* **247** 302

- [29] Apell P, Ljungbert A and Lundqvist S 1984 Non-local optical effects at metal surfaces *Phys. Scr.* **30** 367
- [30] Garcia-Lekue A and Pitarke J M 2001 Energy loss of charged particles interacting with simple metal surfaces *Phys. Rev. B* **64** 035423
- [31] Agranovich V M and Ginzburg V L 1966 *Spatial Dispersion in Crystal Optics and the Theory of Excitons* (London: Interscience)
- [32] Beach R T and Christy R W 1977 Electron-electron scattering in the intraband optical conductivity of Cu, Ag, and Au *Phys. Rev. B* **16** 5277
- [33] Pitarke J M, Silkin V M, Chulkov E V and Echenique P M 2007 Theory of surface plasmons and surface-plasmon polaritons *Rep. Prog. Phys.* **70** 1
- [34] Echenique P M and Pendry J B 1975 Absorption profile at surfaces *J. Phys. C: Solid State Phys.* **8** 2936
- [35] Liebsch A 1993 Surface plasmon dispersion of Ag *Phys. Rev. Lett.* **71** 145
- [36] Rakić A D, Djurić A B, Elazer J M and Majewski M L 1998 Optical properties of metallic films for vertical-cavity optoelectronic devices *Appl. Opt.* **37** 5271
- [37] Rakić A D 1995 Algorithm for the determination of intrinsic optical constants of metal films: application to aluminum *Appl. Opt.* **34** 4755
- [38] Raether H 1988 *Surface Plasmons on Smooth and Rough Surfaces and on Gratings* (Heidelberg: Springer)
- [39] Ciraci C, Pendry J B and Smith D R 2013 Hydrodynamic model for plasmonics: a macroscopic approach to a microscopic problem *Chem. Phys. Chem.* **14** 1109
- [40] Schnitzer O, Giannini V, Maier S A and Craster R V 2016 Surface plasmon resonances of arbitrarily shaped nanometallic structures in the small-screening-length limit *Proc. R. Soc. A* **472** 20160258
- Luo Y, Zhao R and Pendry J B 2014 van der Waals interactions at the nanoscale: the effects of nonlocality *Proc. Natl Acad. Sci. USA* **111** 18422
- Luo Y, Fernandez-Dominguez A I, Wiener A, Maier S A and Pendry J B 2013 Surface plasmons and nonlocality: a simple model *Phys. Rev. Lett.* **111** 093901
- [41] David C and Javier García de Abajo F 2014 Surface plasmon dependence on the electron density profile at metal surfaces *ACS Nano* **8** 9558
- [42] Toscano G, Straubel J, Kwiatkowski A, Rockstuhl C, Evers F, Xu H, Mortensen N A and Wubs M 2015 Resonance shifts and spill-out effects in self-consistent hydrodynamic nanoplasmonics *Nat. Commun.* **6** 7132
- [43] Yan W 2015 Hydrodynamic theory for quantum plasmonics: linear-response dynamics of the inhomogeneous electron gas *Phys. Rev. B* **91** 115416
- [44] Ciraci C 2016 Quantum hydrodynamic theory for plasmonics: impact of the electron density tail *Phys. Rev. B* **93** 205405
- [45] Christensen T, Yan W, Jauho A-P, Solijacic M and Mortensen N A 2017 Quantum corrections in nanoplasmonics: shape, scale and material *Phys. Rev. Lett.* **118** 157402
- [46] Deng H-Y 2018 An analytical dynamical response theory for bounded medium without additional boundary conditions: a unified view of dispersive and non-dispersive models arXiv:1806.08308
- [47] Feibelman P J 1971 Intensity of the infinite-wavelength surface plasmon frequency to the electron density profile *Phys. Rev. B* **3** 220
- [48] Fuchs K 1938 The conductivity of thin metallic films according to the electron theory of metals *Proc. Camb. Phil. Soc.* **34** 100
- [49] Ziman J M 2001 *Electrons and Phonons: The Theory of Transport Phenomena in Solids* (Oxford: Oxford University Press)
- [50] Abrikosov A A 1988 *Fundamentals of the Theory of Metals* (Amsterdam: Elsevier)
- [51] Reuter G E H and Sondheimer E H 1948 The theory of the anomalous skin effect in metals *Proc. R. Soc. A* **195** 338
- [52] Kaganov M I, Lyubarskiy G Y and Mitina A G 1997 The theory and history of the anomalous skin effect in normal metals *Phys. Rep.* **288** 291
- [53] Lawrence W E 1976 Electron-electron scattering in the low-temperature resistivity of the noble metals *Phys. Rev. B* **13** 5316
- [54] Johnson P B and Christy R 1972 Optical constants of the noble metals *Phys. Rev. B* **6** 4370
- [55] Marini A, Sole R D and Onida G 2002 First-principles calculation of the plasmon resonance and of the reflectance spectrum of silver in the GW approximation *Phys. Rev. B* **66** 115101
- [56] It is expected that γ_{residual} for Ag is similar to that for gold. The latter has been measured in several works, e.g. Liu M, Pelton M and Guyot-Sionnest P 2009 Reduced damping of surface plasmons at low temperatures *Phys. Rev. B* **79** 035418
- Bouillard J-S G, Dickson W, O'Connor D P and Wurtz G A 2012 Low-temperature plasmonics of metallic nanostructures *Nano Lett.* **12** 1561
- [57] Rocca M, Biggio F and Valbusa U 1990 Surface-plasmon spectrum of Ag(001) measured by high-resolution angle-resolved electron-energy-loss-spectroscopy *Phys. Rev. B* **42** 2835
- [58] Rocca M, Moresco F and Valbusa U 1992 Temperature dependence of surface plasmons on Ag(001) *Phys. Rev. B* **45** 1399
- [59] Lee K-H and Chang K J 1994 First-principles study of the optical properties and the dielectric response of Al *Phys. Rev. B* **49** 2362
- [60] Powell C J and Swan J B 1959 Effect of oxidation on the characteristic loss spectra of aluminum and magnesium *Phys. Rev.* **116** 81
- Powell C J and Swan J B 1959 Origin of the characteristic electron energy losses in magnesium *Phys. Rev.* **115** 869
- [61] Knight M W, King N S, Liu L, Everitt H O, Nordlander P and Halas N J 2014 Aluminum for plasmonics *ACS Nano* **8** 834
- [62] Sinvani M, Greenfield A J, Bergmann A, Kaveh M and Wisner N 1981 Effect of annealing on the temperature dependence of the electrical resistivity of aluminium *J. Phys. F: Met. Phys.* **11** 149
- [63] Ribot J H J M, Bass J, van Kempen H and Wyder P 1979 Further evidence for electron-electron scattering in aluminum *J. Phys. F: Met. Phys.* **9** L117
- [64] Beck D E 1991 Interband contribution to the long-wavelength damping of the surface plasmon *Phys. Rev. B* **43** 12611
- [65] Iranzo D A *et al* 2018 Probing the ultimate plasmon confinement limits with a van der Waals heterostructure *Science* **360** 291
- [66] Aminov K L and Pedersen J B 2001 Quantum theory of high-energy electron transport in the surface region *Phys. Rev. B* **63** 125412
- [67] Garcia-Moliner F and Flores F 1979 *Introduction to the Theory of Solid Surfaces* (Cambridge: Cambridge University Press)
- [68] Gervasoni J L and Arista N R 1992 Energy loss and plasmon excitation during electron emission in the proximity of a solid surface *Surf. Sci.* **260** 329
- [69] Yubero F, Sanz J M, Ramskov B and Tougaard S 1996 Model for quantitative analysis of reflection-electron-energy-loss spectra: angular dependence *Phys. Rev. B* **53** 9719
- [70] Serway R A *Principles of Physics* 2nd edn (London: Saunders College)